Chemical Engineering Report Series
Kemian laitetekniikan raporttisarja No. 49
Espoo 2005

MODELLING A PROCESS FOR DIMERISATION OF 2-METHYLPROPENE

Tuomas Ouni

TEKNILLINEN KORKEAKOULU
TEKNISKA HÖGSKOLAN
HELSINKI UNIVERSITY OF TECHNOLOGY
TECHNISCHE UNIVERSITÄT HELSINKI
UNIVERSITE DE TECHNOLOGIE D'HELSINKI

Chemical Engineering Report Series
Kemian laitetekniikan raporttisarja No. 49
Espoo 2005

MODELLING A PROCESS FOR DIMERISATION OF 2-METHYLPROPENE

Tuomas Ouni

Dissertation for the degree of Doctor of Science in Technology to be presented with due permission for public examination and debate in Auditorium Ke 2 at Helsinki University of Technology (Espoo, Finland) on the 19th of November, 2005, at 12 o'clock.

Helsinki University of Technology
Department of Chemical Technology
Laboratory of Chemical Engineering and Plant Design

Teknillinen korkeakoulu
Kemian tekniikan osasto
Kemian laitetekniikan ja tehdassuunnittelun laboratorio

Distribution:
Helsinki University of Technology
Laboratory of Chemical Engineering and Plant Design
P. O. Box 6100
FIN-02015 HUT
Tel. + 358-9-4511
Fax. +358-9-451 2694
E-mail: Tuomas.Ouni@hut.fi

ISBN 951-22-7925-8
ISSN 1236-875X

Otamedia Oy
Espoo 2005

ABSTRACT

Isooctane can be used to replace methyl-*tert*-butyl ether (MTBE) as a fuel additive. Isooctane is hydrogenated from isooctene, which is produced by dimerizing 2-methylpropene. In dimerization, two 2-methylpropene molecules react on ion-exchange resin catalyst to produce isooctene isomers (2,4,4-trimethyl-1-pentene, 2,4,4-trimethyl-2-pentene). Presence of 2-methyl-2-propanol (TBA) improves reaction selectivity. Trimers and tetramers are formed as side products. Water and alkenes have reaction equilibrium with corresponding alcohols.

The process configuration for isooctene production is a side reactor concept, and consists of reactor part, separation part (distillation tower) and a recycle structure (Figure 1). Units of miniplant at Helsinki University of Technology imitates the actual units of the isooctene production line in smaller scale, providing valuable information about the process and about the behaviour of individual units, as well as about the dynamics and operability of the process.

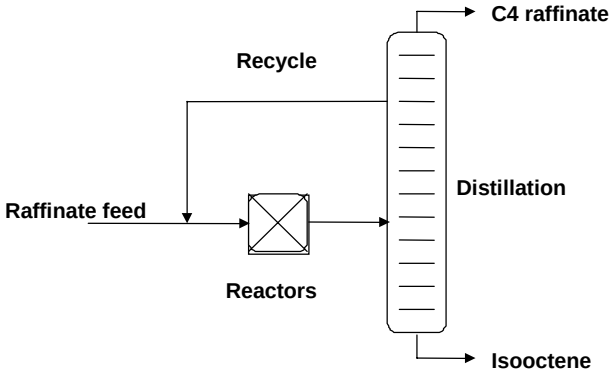

Figure 1. Process configuration of the dimerisation section of NExOCTANE process.

Ideology behind Miniplant is to separate thermodynamical models from hardware-specific models, so that they could be used as such in other contexts, e.g. in industrial scale. In the specific case of 2-methylpropene dimerisation the key thermodynamical models are vapour-liquid and liquid-liquid equilibrium as well as reaction kinetics. Hardware specific models include distillation column with spring-shaped packings and tubular catalytic reactor with heating coil and a thermowell. Developing these models through experiments and simulations was the primary target of this work.

PREFACE

The work described in this thesis was carried out in the Laboratory of Chemical Engineering and Plant Design, Helsinki University of Technology, between June 2001 and October 2005. Funding from the National Technology Agency of Finland (Tekes) and Fortum Oil and Gas Oy is gratefully acknowledged. Additionally, the Academy of Finland is thanked for its support through the Graduate School in Chemical Engineering (GSCE).

I am most grateful to Prof. Juhani Aittamaa for his guidance throughout the preparation of this thesis.

Senior colleagues Dr. Kaj Jakobsson, Dr. Juha-Pekka Pokki, Dr. Petri Uusi-Kyyny and Petri Lievo are gratefully acknowledged for their invaluable help with the experimental work and the calculations.

Co-authors Maija Honkela, Antti Pyhälahti, Anna Zaytseva and Aspi Kolah are warmly thanked for their ideas and contributions.

Sirpa Aaltonen and Lasse Westerlund are warmly thanked for helping with administrative issues.

Furthermore, I want to express my gratitude to my parents and my friends, who have supported me in my work throughout the preparation of this thesis.

Finally my warmest thanks to Reetta,

Espoo, 19.10.2005

Tuomas Ouni

LIST OF PUBLICATIONS

This thesis is based on following publications (Appendices I-V), which are referred to in the text by their roman numerals:

I Ouni, T., Jakobsson, K., Pyhälahti, A. and Aittamaa J., Enhancing productivity of side reactor configuration through optimizing the reaction conditions. *Chem. Eng. Res. Des.*, 82 (**2004**) 167-174.

II Ouni T., Uusi-Kyyny P., Pokki J.-P. and Aittamaa J., Isothermal Vapor Liquid Equilibrium for Binary 2-Methylpropene + Methanol to Butanol Systems. *J. Chem. Eng. Data* 49 (**2004**) 787-794.

III Honkela, M., Ouni, T. and Krause, O., Thermodynamics and kinetics of the dehydration of *tert*-butyl alcohol. *Ind. Eng. Chem. Res*, 43 (**2004)** 4060-4065.

IV Ouni T., Honkela M., Kolah A. and Aittamaa J., Isobutene dimerisation in a miniplant-scale reactor. Accepted for publication in *Chem. Eng. Process* in *October 2005.*

V Ouni T., Zaytseva A., Uusi-Kyyny P., Pokki J.-P. and Aittamaa J., Vapour-liquid equilibrium for the 2-methylpropane + methanol, +ethanol, +2-propanol, +2-butanol and +2-methyl-2-propanol systems at 313.15 K. *Fluid Phase Equilibr.* 232 (**2005**) 90-99.

Author’s contribution to the appended publications

I The author performed the calculations and wrote the paper with the co-authors.

II The author made the measurements with the co-authors, performed the calculations and partly wrote the paper.

III The author assisted in the calculations, in evaluating the results for the paper and in writing the paper.

IV The author made the experiments, performed the calculations and wrote the paper with the co-authors.

V The author made the experiments, performed the calculations and wrote the paper with the co-authors.

1 INTRODUCTION

Scale-up method relies essentially on construction of a series of larger and larger plants starting from the laboratory scale until the full production scale has been achieved. In the most rudimentary form of this method, no complex models are applied, but the scale-up means essentially extrapolation of the previous design to a larger scale. The so-called scale-up rules are essentially similarity rules applied for this extrapolation. Usually the rules do not allow large extrapolation steps, thus several intermediate size plants are needed and it easily takes 5-10 years to develop a process out of scratch. On the other hand, scale-up is a very robust way of process development, because every aspect of designing and operating the plant is usually encountered during the development work.

The development and the design of new processes are today extensively based on mathematical modeling and simulation. Through simulations various process options can be evaluated at an early stage in the development. The entire process is modeled through combining individual unit operation models.

The various physical and chemical phenomena occurring in each process unit (reaction kinetics, heat and mass transfer, phase equilibrium, hydraulics) have to be known. Reactors for instance require kinetic models that describe how local concentrations and temperature affect the reaction rates. Separation processes require knowledge of mass transfer and phase equilibrium (vapour/liquid, liquid/liquid).

The model-based approach is based on constructing a mathematical model of the process, instead of pilot plants. Only experiments necessary for collecting physical and chemical data not available from other sources are performed. After gathering all necessary data, a model of the whole process is set up and the plant is designed and optimised as a model using a computer.

An obvious benefit of model-based approach is avoiding the costly and time consuming construction and operation of pilot plants. On the other hand, the requirements set on the quality of the experiments performed for gathering the data for modelling are stringent and modelling work itself requires significant resources and time. However, the most dangerous pitfall is that some important factor may be overlooked in the modelling work.

The miniplant concept tries to combine the best properties of both these development routes. According to the miniplant concept, substantial part of the process development is based on modelling, so that the process concept can be set up without pilot work. Then a pilot-plant as small as possible for achieving meaningful results is constructed and the validity of the models applied is tested against the results achieved.

With the currently available equipment, the size of miniplant is between laboratory scale and pilot scale equipment, typical feed being 0.2-3 kg/h. Miniplant hardware costs, as well as utility and chemical costs are usually moderate which makes the technology available for e.g. universities and small research institutes. Also safety issues are more easily handled with small-scale equipment.

One important field of application for a miniplant is the study of recycles. The build-up of an unwanted component that might be unnoticed in laboratory reactor experiments can be found in a miniplant test run, provided that all intended recycles are present, and that the process is allowed to reach a steady state.

Using a series of consecutive experiments in increasing equipment size as a scale-up method would give detailed knowledge about the process behaviour and possible build-ups in the recycle structure. To achieve this knowledge through miniplant experiments and process simulation requires refined thermodynamical models and accurate, tailor-made models for the small-scale miniplant equipment. The benefit with miniplant experiments and detailed modeling would of course be significant savings in process development time and resources.

Process for dimerising 2-methylpropene provides an outstanding example how the miniplant concept can be successfully exploited. The dimerisation product of 2-methylpropene, 2,4,4-trimethyl pentene, can be hydrogenated into isooctane (2,4,4-trimethyl pentane) that can be used to replace methyl-*tert*-butyl ether (2-methoxy-2-methylpropane, MTBE) as a gasoline additive.

MTBE, once the blue eye chemical of the chemical industry and in the last decade having been labelled as the fastest growing chemical in the world, is currently under tremendous scrutiny and pressure from environmental regulation agencies in the United States to decrease or totally eliminate its use from the gasoline pool. Since the last 20 years MTBE has been blended into gasoline and is an efficient way for refineries to meet the regulations for oxygenated and reformulated gasoline.

Groundwater and surface water contamination associated with MTBE from leaking underground tanks is the cause of the current controversy as between 5 to 10% of ground water in areas using MTBE blended gasoline have detectable levels of MTBE. As a consequence, a ban on MTBE took effect from January 2004 in California after granting a one-year waiver, and several other states in USA are predicted to follow California's action.

Of the various potential substitutes to MTBE, isooctane is one of the leading contenders. Isooctane is synthesized from 2-methylpropene by selective dimerization to form isooctene, followed by hydrogenation. In locations where the olefin content of gasoline is not limited, isooctene can be directly blended into the gasoline pool. Isooctane has numerous advantages, its properties being high octane number and zero content of aromatics, sulphur and olefins, low vapour pressure and for the MTBE producing refineries it has the decisive advantage of necessating a moderate revamp of the already existing refinery facilities. Moreover MTBE has been a major consumer of 2-methylpropene from C4 hydrocarbon stock and its phase out will cause a major decline in the downstream consumption of 2-methylpropene from fluid catalytic cracking and steam cracking product streams.

Scharfe (1973) studied the dimerisation of 2-methylpropene (2-methylpropene) into 2,4,4-trimethylpentene (isooctene) in presence of a solid ion exchange resin catalyst. Tri- and tetraisobutenes were formed as side products. The feed to reactors, coming from gas fields through n-butane to isobutane isomerization and dehydrogenation processes, consists of ~40 % 2-methylpropene, the rest being short (C3-C5) aliphatic or olephinic hydrocarbons. Honkela and Krause (2003) studied the use of *tert*-butyl

alcohol (2-methyl-2-propanol, TBA) feed as selectivity controlling agent. According to their study, without TBA the reaction kinetics favour forming larger, C12 and C16 oligomers of 2-methylpropene.

Oil refinery feed for dimerization process is a mixture of C_4-alkene isomers. The feed originates either from gas fields, or from fluid catalytic cracking (FCC) process, where heavy hydrocarbons of oil are cracked into shorter ones. The C4 alkane coming from the gas fields is mainly n-butane, which first has to be isomerized to isobutane and then further dehydrogenated into 2-methylpropene. Prepared this way, the feed consists of around 50 % 2-methylpropene and 50 % isobutane, with small amounts of other short alkanes and alkenes. The FCC produces a mixture of short hydrocarbons containing (15 to 20) % 2-methylpropene.

The product stream from the reactor train, which in addition to the feed components has oligomers of 2-methylpropene in it, is further led to distillation column. The desired product(s), the oligomers, are separated from lighter hydrocarbons, TBA and water, that has formed as a product of TBA decomposition. TBA and unreacted 2-methylpropene are recycled back to the reactor train, whereas the light C3-C4 hydrocarbons are purged out of the system from the top of the column.

2 VAPOUR-LIQUID EQUILIBRIUM

Vapour-liquid equilibrium is generally modelled using either state equations for both gas and liquid phase, or using activity coefficient model for the liquid phase and state equations for the vapour phase. Generally it can be said that activity coefficient models are better in predicting the behaviour of strongly non-ideal systems, but on the other hand they often need experimental data in order to be accurate. Molecular interactions in the gas phase are usually weak, and no strong nonidealities exist. Therefore the gas phase may safely be treated with state equations.

In a system, where there are alcohols and water present in a hydrocarbon-rich mixture, polar components such as alcohols cause strong nonidealities to exist, and it is necessary to model the liquid phase with activity coefficient model. Models such as UNIQUAC, NRTL and Wilson are widely used for this kind of systems. Of these, Wilson method is known as the most suitable for predicting hydrocarbon-alcohol interactions. The downside of these models is that they need experimental data for each binary interaction in the multicomponent system. When the number of components in the system increases, the amount of binary VLE data needed becomes rapidly very large. Therefore experimental VLE-data is usually acquired through measurements or from literature for the key component binaries only, and predictive methods are used to fill in the remaining gaps in the parameter matrix.

Group contribution methods, such as UNIFAC and ASOG, predict the phase equilibria by treating the liquid phase as a mixture of structural groups. The number of structural groups is of course considerably smaller than number of compounds, and parameters for interactions between structural groups can be fitted and used universally. Currently one of the most applied and the most rigorous group contribution method, developed by Weidlich and Gmehling (1987), is modified UNIFAC (Dortmund), which has the advantage over traditional UNIFAC that it can predict temperature dependence of the activity coefficients correctly and it has improved combinatorial part for strongly asymmetric systems.

When the group contribution methods are not adequate, the liquid phase is here modelled with the temperature dependent Wilson equation. In the method of Wilson (1964), the activity coefficients γ_i in liquid phase for a mixture of m components are calculated from

$$\ln \gamma_i = -\ln\left(\sum_{j=1}^{m} x_j \Lambda_{ij}\right) + 1 - \sum_{k=1}^{m} \frac{x_k \Lambda_{ki}}{\sum_{j=1}^{m} x_j \Lambda_{kj}}, \tag{2.1}$$

where Λ_{ij} are binary interaction parameter for components i and j in the mixture. Λ_{ii}'s have a value of 1. Temperature effect on the activity coefficients can be incorporated by calculating Λ_{ij}'s from

$$\Lambda_{ij} = \frac{V_j^L}{V_i^L} \exp\left(-\frac{\lambda_{ij}}{RT}\right), \tag{2.2}$$

where V_i^L is pure component molar volume for component i and λ_{ij}'s are the fitted parameters. For λ_{ii}'s, a value of 0 is assigned. Furthermore, the temperature dependence can be expanded by calculating λ_{ij}'s from

$$\lambda_{ij} = a_{ij} + b_{ij} T \tag{2.3}$$

where a_{ij} and b_{ij} are now the parameters to be fitted.

The Soave-Redlich-Kwong equation of state with quadratic mixing rule for the attractive parameter and a linear mixing rule for the covolume parameter for the evaluation of vapor phase fugacity coefficients is used throughout this work to treat the vapour phase non-idealities. The binary interaction parameter in the quadratic mixing rule was set to zero.

Critical temperatures, critical pressures, acentric factors and liquid molar volumes were acquired from the DIPPR database. The vapour pressure equation parameters were chosen through comparing the measured values and the values calculated from different sources. The vapour pressure values calculated from the DIPPR correlation were closest to our measurements and were thus chosen to represent the vapour pressure behaviour, except for the 2,4,4-trimethyl-1-pentene, for which the Antoine equation was used. Absolute or relative differences between measured and calculated pressures were used as objective function for optimisation algorithms of Nelder and Mead (1965) and Davidon (1975).

Honkela and Krause (2004) and Honkela *et al*. (2004), in their experimental study of the kinetics of 2-methylpropene dimerisation and other reaction closely coupled with this reaction (III), used Dortmund modified UNIFAC in calculating the liquid phase activity coefficients for their modeling work. The same thermodynamic method is preferred in reactor simulations as is used in the kinetic modelling. Even though there are methods that are more suitable for hydrocarbon-alcohol systems, and that are based on experimental data, such as the Wilson method, preliminary simulations

indicated that the results obtained by Dortmund modified UNIFAC correspond better to the measurements than the ones made with other methods. Therefore Dortmund-modified UNIFAC is used in the reactor simulations described more in detail in chapter 3 and 4.

In the component matrix for the process of 2-methylpropene dimerisation, three main binary interaction groups exist:

- Hydrocarbon-hydrocarbon interactions,
- Hydrocarbon-alcohol interactions and
- Hydrocarbon-water interactions

Each group has their own characteristics, and following chapters summarise the treatment in terms of activity coefficient calculations for each type of interaction.

2.1. Hydrocarbon-hydrocarbon interactions

Hydrocarbon-hydrocarbon interactions are close-to-ideal. Therefore the prediction of their binary interactions in terms of activity coefficient does not necessarily require experimental data, but most predictive methods, such as Dortmund-modified UNIFAC, can perform the task instead. For the present system, consisting of C3 and longer hydrocarbons, the number of hydrocarbon-hydrocarbon binaries is large, and no sufficient experimental VLE data is available for most binaries. When parameters for Wilson method are needed, Dortmund-modified UNIFAC can be used to produce adequate VLE data by fixing liquid phase composition and pressure or temperature and letting Dortmund-modified UNIFAC calculate the liquid phase activity coefficient. Data produced this way has proved to be sufficient in predicting the behaviour of hydrocarbons in reactor system.

Since hydrocarbon-hydrocarbon interactions are close-to-ideal, vapour pressures define their separation. Therefore, in addition to accurate prediction of activity coefficients, the calculation of precise vapour pressures is vital. Correlations for vapour pressures are widely available, perhaps most prominent ones being the methods of Antoine and Wagner. The method of Wagner is applicable for a larger temperature range, but parameters for Wagner method are more scarcely available than for the method of Antoine. The parameters for vapour pressure correlations may be obtained from books by Yaws (1999), Perry (1997) or Reid (1987), and the applicability of them at the condition range at hand may be determined by comparison to measured data.

2.2. Hydrocarbon-alcohol interactions

Hydrocarbon-alcohol systems are non-ideal, and experimental data is needed to accurately calculate the activities for such systems. In the reaction system, TBA is the alcohol that exist in largest concentrations throughout the process. However, since the system contains water and C3-C5 olefins, other C3-C5 alcohols are likely to be present in some level. At HUT laboratory of chemical engineering, VLE has been measured for most C4 parafin – C1-C4 –alcohols. The author has reported VLE measurements for 2-methylpropene - C1-C4 –alcohol (II) and isobutane - C1-C4 –

alcohol (V) binaries. Following text summarises the experimental procedure and the results of those measurements. The results have been used in fitting parameters for Wilson method for VLE predictions.

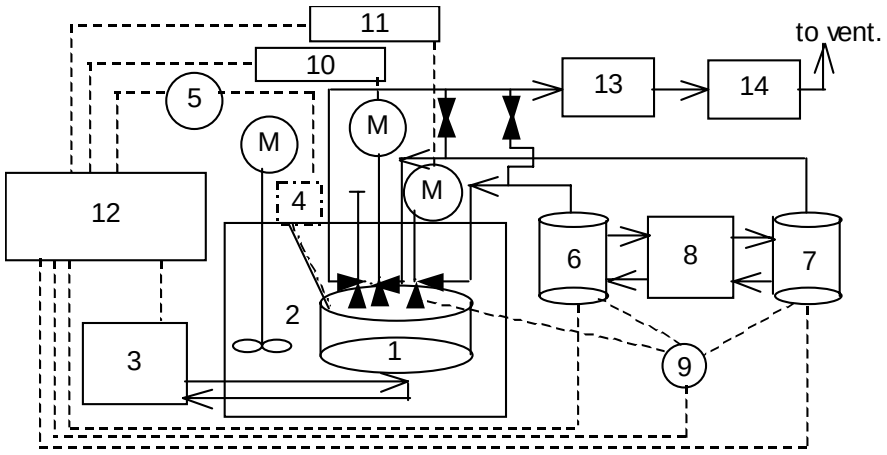

Figure 2. Schematic figure of the automated apparatus: 1, equilibrium cell with a magnetic stirrer; 2, 70 dm^3 water bath; 3, circulator thermostat; 4, electrically traced pressure transducer connected to the equilibrium cell with electrically traced 1/16 inch tubing; 5, pressure display; 6, 7, syringe pumps; 8, circulator thermostat; 9, temperature display; 10, 11, stepper motor interface card; 12, PC with a SmartIO C168H card at PCI bus; 13, liquid nitrogen trap; 14, vacuum pump.

Details of the VLE apparatus are presented by Uusi-Kyyny *et al.* (2002). The experimental set-up is presented in Figure 2.

For each measured system an identical measuring procedure was followed. The composition range was measured in two parts; from the both ends of pure components to an approximately equimolar mixture. Injection volumes were optimised so that the equilibrium cell became nearly filled with mixture in both parts of the measurement. This was done to improve the measurement accuracy of overall compositions in the equilibrium cell. The syringe pumps were operated in constant pressure mode (900 kPa) to ensure the accuracy of the volume measurement, to prevent the contamination of degassed components and to keep 2-methylpropene in liquid phase.

A model by Thomson *et al.* (1982) was used to take into account the pressure effects on the liquid densities in the syringe pumps. The temperatures of the syringe pumps were measured. The cell content and the bath were mixed continuously during the measurements.

Pure component vapour pressures and 23 to 26 equilibrium points were measured in each run. At first, component 1 was introduced into the cell and its vapour pressure was measured. The unchanged pressure after a second addition of the first component into the cell indicated the success of the degassing. The vapour pressure would rise due to incomplete degassing of the component as a result of dissolved gases in the equilibrium cell. After the vapour pressure measurement of component 1 a predetermined volume of component 2 was added to the equilibrium cell. The cell content was mixed with a magnetic mixer and the cell was let to equilibrate for approximately 30 min. The additions of component 2 were continued until the target

composition was reached and cell became nearly filled with the mixture. The emptying and the evacuation of the equilibrium cell ended the first part of the measurement. Measuring the other side of the isotherm was initiated by injecting the pure component 2 and checking its vapour pressure. The additions of component 1 were continued to the target composition. The success of the run could be verified by comparing the coincidence of the cell pressures as a function of total composition when the different sides of the isotherm meet at the mole fraction of approximately 0.5.

The method proposed by Barker (1953) was used to convert the total amount of moles fed in to the cell into mole fractions in both vapour and liquid phase. The method of Barker data reduction assumes that there is an activity coefficient model that can predict the bubble point pressure in higher accuracy than the experimental error of the measured total pressure. Barker's method is an iterative method, which needs vapour phase fugacities and liquid phase activities to be calculated. Liquid phase activity coefficients were obtained using Legendre polynomial, which due to its flexible nature is suitable for accurately predicting non-ideal behaviour of the liquid phase. To avoid overfitting, as few parameters were used in Legendre polynomials as was necessary in terms of successful data reduction.

Tables 1 and 2 summarise the results of the VLE measurements performed by the author. Table 1 presents the fitted parameters, average pressure residuals indicating the bias between measured and model predicted pressures and average absolute pressure residuals indicating the accuracy of the model-given pressures for 2-methyl propane and C1-C4 alcohols at 313 K. Table 2 gives a similar presentation for the 2-methyl propene – C1-C4 alcohol experiments.

Table 1. Activity coefficient model parameters, Legendre, Wilson, NRTL, UNIQUAC. Data regressed with the Legendre-polynomials, average pressure residual Δp, absolute average pressure residual $|\Delta p|$, 2-methylpropane + methanol at 313.15 K (system 1), 2-methylpropane + ethanol at 313.15 (system 2), 2-methylpropane + 2-propanol at 313.15 (system 3), 2-methylpropane + 2-butanol at 313.15 (system 4), 2-methylpropane + 2-methyl-2-propanol at 313.15 (system 5).

	System 1	System 2	System 3	System 4	System 5
Legendre, $a_{1,0}$	2.5899	1.9446	1.9046	1.7052	1.4945
Legendre, $a_{2,0}$	0.34409	0.435	0.51203	0.53657	0.47491
Legendre, $a_{3,0}$	0.47737	0.2212	0.3248	0.28564	0.29079
Legendre, $a_{4,0}$	0.16949	0.079135	0.17313	0.17481	0.14694
Legendre, $a_{5,0}$	0.11144	0.02945	0.098876	0.078351	0.077412
Legendre, $a_{6,0}$	0.054445	1.9446	0.047	0.047236	0.038301
Legendre, $a_{7,0}$	0.027639	0.435	0.024753	0.015036	0.01905
Legendre, $a_{8,0}$	0.012643	0.2212	0.0081365	0.0081676	0.006954
Legendre, $a_{9,0}$	0	0.079135	0.0038975	0	0.0032083
Legendre, $a_{10,0}$	0	0.02945	0	0	0
Δp/kPa	0.07	0.04	0.02	0.02	0.00
$\|\Delta p\|$/kPa	0.12	0.07	0.09	0.09	0.11
	System 1	System 2	System 3	System 4	System 5
Wilson, λ_{12}/ (J/mol)	2257.77	1349.758	1063.131	988.534	493.084
Wilson λ_{21}/ (J/mol)	10770.45	8760.878	6649.363	5761.937	5143.391
Δp/kPa	0.56	0.13	1.27	-1.26	-1.91
$\|\Delta p\|$/kPa	3.30	1.42	2.07	2.28	3.8
NRTL, λ_{12}/ K	769.17	725.11	639.66	610.47	563.31
NRTL, λ_{21}/ K	563.6	384.79	290.8	247.6	222.86
NRTL, $\alpha_{12}=\alpha_{21}$	0.43246	0.45855	0.51084	0.56373	0.66941
Δp/kPa	-1.94	-0.62	1.13	-1.00	0.85
$\|\Delta p\|$/kPa	3.40	3.27	2.94	2.56	1.6
UNIQUAC, λ_{12}/ K	634.14	452.8	320.12	156.26	229.35
UNIQUAC, λ_{21}/ K	34.462	-26.642	-33.776	22.318	-40.541
Δp/kPa	-5.87	5.24	5.83	-4.46	-4.14
$\|\Delta p\|$/kPa	15.56	10.8	8.10	6.32	6.26

Table 2. Activity coefficient model parameters for Legendre, Wilson, NRTL and UNIQUAC. Data regressed with the Legendre-polynomials, average pressure residual Δp, absolute average pressure residual |Δp|, 2-methylpropene + methanol at 323.15 K (System 1), 2-methylpropene + ethanol at 323.15 K (System 2), 2-methylpropene + 2-propanol at 323.15 K (System 3), 2-methylpropene + 2-butanol at 323.15 K (System 4), 2-methylpropene + 2-methyl-2-propanol at 313.15 K (System 5) and 2-methylpropene + 2-methyl-2-propanol at 322.77 K (System 6)

	System 1	System 2	System 3	System 4	System 5	System6
Legendre, $a_{1.0}$	2.2575	1.9415	1.6188	1.4108	1.3002	1.2343
Legendre, $a_{2.0}$	0.3350	0.4457	0.4116	0.3964	0.4019	0.3536
Legendre, $a_{3.0}$	0.2894	0.2410	0.2005	0.1762	0.2025	0.1763
Legendre, $a_{4.0}$	0.0761	0.0835	0.0741	0.0625	0.0603	0.0530
Legendre, $a_{5.0}$	0.0286	0.0359	0.0260	0.0199	0.0233	0.0228
Δp / kPa	0.132	0.292	0.216	-0.026	0.252	-0.014
|Δp| / kPa	0.656	0.734	0.689	0.369	0.555	0.309
	System 1	System 2	System 3	System 4	System 5+6	
Wilson, λ_{12} / J·mol^{-1}	1123.624	778.0515	735.289	749.6408	1700.039	
Wilson, λ_{21} / J·mol^{-1}	9234.105	7977.172	5780.05	4757.432	1857.574	
Wilson, λ_{12} / J·K^{-1}·mol^{-1}					-3.9549	
Wilson, λ_{21} / J·K^{-1}·mol^{-1}					8.089727	
Δp / kPa	0.026	0.719	0.651	1.484	1.675	
|Δp| / kPa	1.805	1.892	2.571	2.565	4.001	
NRTL, λ_{12} / K	623.31	624.86	536.5	509.33	338.57	
NRTL, λ_{21} / K	395.69	244.57	149.31	87.568	-198.63	
NRTL, λ_{12}					0.4408	
NRTL, λ_{21}					0.7763	
NRTL, $\alpha_{12} = \alpha_{21}$	0.4	0.4	0.4	0.4	0.4	
Δp / kPa	2.464	2.972	2.660	2.820	2.543	
|Δp| / kPa	7.823	6.370	5.603	5.235	6.167	
UNIQUAC, λ_{12} / K	614.81	437.58	295.04	191.45	151.54	
UNIQUAC, λ_{21} / K	9.091	-39.681	-37.263	-15.511	6.713	
UNIQUAC, λ_{12}					0.167	
UNIQUAC, λ_{21}					-0.130	
Δp / kPa	3.876	5.271	3.260	-0.771	2.627	
|Δp| / kPa	11.198	9.152	6.824	6.837	5.743	

In II and V, azeotropic behaviour was observed for following binaries at given conditions.

- 2-methylpropene (1) + methanol (2) at point $x_1 = 0.941$, T = 323.14 K and p = 623.1 kPa,
- 2-methylpropane (1) +methanol (2) at $x_1 = 0.947$, T = 313.06 K and p = 548.25 kPa and

- 2-methylpropane (1) +ethanol (2) at $x_1 = 0.990$, T = 313.08 K and p = 531.34 kPa.

These findings are well in line with the observations reported earlier by Leu *et al.* (1992), Zabaloy *et al.* (1992, 1993), Fischer *et al.* (1996) and Verrazzi and Kikic (1996).

2.3. Hydrocarbon-water interactions

Water-hydrocarbon interactions are extremely non-ideal, and the presence of water in a hydrocarbon mixture is likely to produce a liquid-liquid phase split. Presence of alcohols increases the solubility of water in the mixture. VLE data for hydrocarbon-water systems is impractically difficult to measure because of this, and therefore the parameters for calculating the activity coefficients of water must be obtained in a different manner. Infinite dilution activity coefficients provide one option of doing this.

Solubilities and LLE data may provide means to predict the behaviour of water in a hydrocarbon-alcohol-water mixture. Some of the activity coefficient calculation methods (UNIQUAC, NRTL, T-K-Wilson but not traditional Wilson) can handle LLE data as well. The results of predicting liquid phase activities for VLE based on LLE-data are not very encouraging up to this date; reliable VLLE data is scarcely available for water-alcohol-hydrocarbon systems. However, the solubility data obtained from LLE measurements may be used in predicting the phase behaviour of water: the inverse of the molar solubility of water into hydrocarbon gives a rough estimate on the infinite dilution activity coefficient for water. The same applies for the other end of the solubility range.

Considering the difficulties in predicting the VLE of water and hydrocarbons, it is fortunate that in view of our separation process, the accuracy of the activity coefficients is, although important, not vital. What is important, though, is to know the solubilities of water at different conditions, knowing the azeotropic behaviour of water with alcohols and predicting large enough activity coefficients for water. In terms of reactor design, the need for accurate activities is stronger, especially if water is participating in the reactions considered. Then the proceeding of the reaction may be determined by the activity of the water.

2.4. Comparison between methods for calculating VLE

The performance of the VLE model developed will be tested in chapter 4.2 against a multicomponent distillation experiment. However, there are also other ways of judging the reliability and accuracy of a VLE model.

One way of comparing VLE models is to look at predicted azeotropic compositions for component binaries at different temperatures and pressures. This is done here for the following binaries that are known to present azeotropic behaviour:

- TBA – water and
- TBA - TMP-1.

Both of these azeotropes are important for the operation of the distillation system. TBA should in order for it to exit the column with recycle, be adjusted so that its concentration has a maximum at the stage where the recycle stream is taken out. Controlling the TBA levels in the column with normally fluctuating feed requires accurate knowledge about the behaviour of TBA-hydrocarbon binaries. Figures 3a and 3b show the azeotropic composition for water and TMP-1 plotted against temperature, ranging from 50 °C to 200 °C. The azeotropic compositions given by Wilson method and UNIFAC are compared to the measured ones, reported by Gmehling *et al.* (1994), Baer and Quitzsch (1974) and by Uusi-Kyyny *et al.* (2001).

For TMP-1 – TBA –binary, the prediction of Wilson method follows measured values closely. At moderate temperatures, UNIFAC prediction approaches the Wilson predictions. At higher temperatures the predictions differ significantly from each other. Wilson method gives a linearly decreasing correspondence for $x_{az,TMP\text{-}1}$ vs. temperature, whereas UNIFAC predicts a rise for azeotropic mole fraction of TMP-1 when the temperature is increased above 150 °C.

For TBA – water binary, azeotropic curve determined by Wilson method follows quite closely the average of literature azeotropic data. The shape of the x_{az} vs. T -curve is similar for Wilson method and UNIFAC, but UNIFAC predicts 5-10 mole % higher azeotropic mole percentages for water than Wilson.

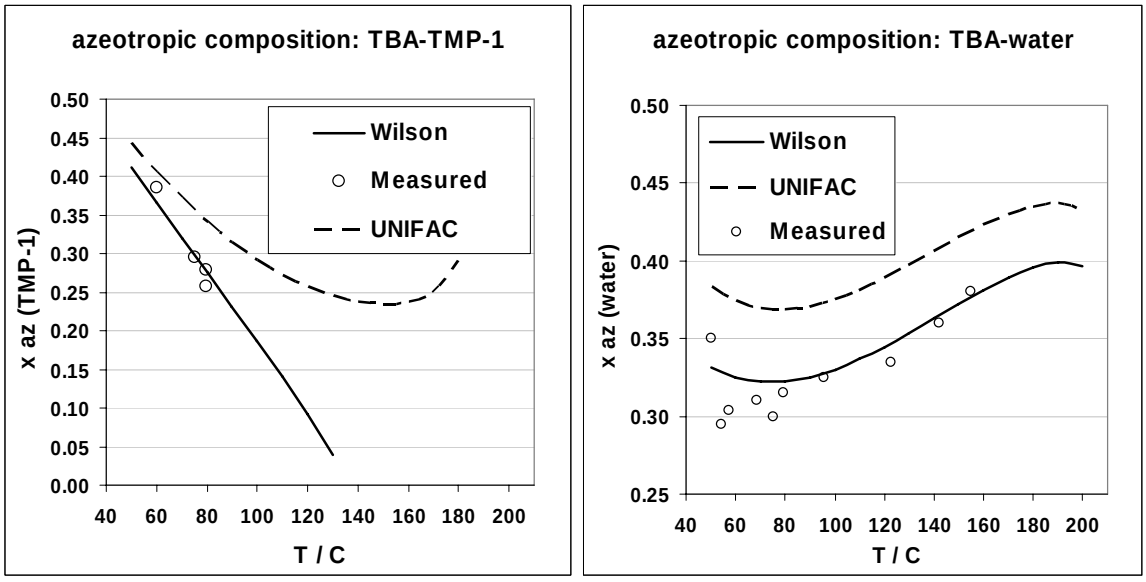

Figure 3a and 3b. Azeotropic composition vs. temperature as given by measurements, Wilson method and UNIFAC for TBA - TMP-1 and TBA – water binaries.

3 REACTIONS AND KINETIC MODEL

The dimerization of 2-methylpropene (isobutene, IB) has been widely investigated as a side reaction in IB etherification processes, such as the synthesis of MTBE, investigated by Vila *et al.* (1994) and isopropyl *tert*-butyl ether synthesis, studied by Tejero *et al.* (1997). Studies have also been carried out on simultaneous dimerization

and etherification by Di Girolamo *et al.* (1997) and Di Girolamo and Marchionna (2001).

In IB dimerization, two IB molecules react with each other on an acid catalyst, such as an ion-exchange resin. Side reactions include the formation of triisobutenes (TRIBs) and higher oligomers. If a polar component is added to increase the selectivity, various etherification and dehydration reactions occur as well. With *tert*-butyl alcohol (TBA; 2-methyl-2-propanol) added, the selectivity is increased without ether formation. The use of other polar components such as ethanol and 2-propanol has been reported by Di Girolamo and Marchionna (2001), but these also form ethers.

Honkela and Krause (2004) studied IB dimerization catalyzed with an ion exchange resin with TBA as the selectivity-enhancing component. The catalyst is an acidic ion-exchange resin consisting of a styrene-divinylbenzene-based support to which sulfonic acid groups had been added as active sites. It was obtained from Rohm and Haas and partially pre-dried before use. The average particle size $d_{p,ave}$ for the catalyst was 0.0008 m and it had a bulk density of 850 kg/m^3.

Ion exchange resins have a tendency to absorb water and other polar components in them. Studies by Kawase *et al.* (1996) and Mazzotti *et al.* (1996) in chromatographic reactors have indicated that in addition to the adsorption of chemical species on the active sites of the catalyst, molecules may be absorbed into the catalyst matrix. The reaction fluid is in equilibrium with the catalyst in terms of water and TBA, component activities in the liquid phase and the catalyst phase defining the sorption equilibrium.

Furthermore, it is also possible that the absorption into the resin occurs from another liquid phase. Pilipenko *et al.* (1970) studied LLE for the system 2-methylpropene-water-TBA, and according to their results, the second liquid phase occurs even at trace water concentrations. However, the water-rich phase contains no more than 7 wt-% of TBA at any circumstances. Honkela *et al.* (III) did not observe a second liquid phase when they conducted their experiments for TBA decomposition.

3.1. Dimerisation of 2-methylpropene

Isobutene is dimerised into diisobutene (DIB) according to scheme 1. Further oligomerisation is assumed to take place according to scheme 2.

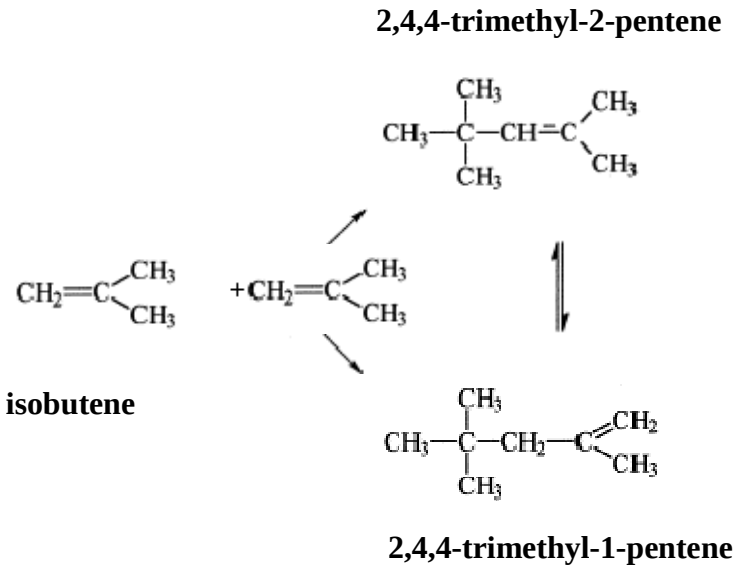

Scheme 1. Dimerisation of 2-methylpropene

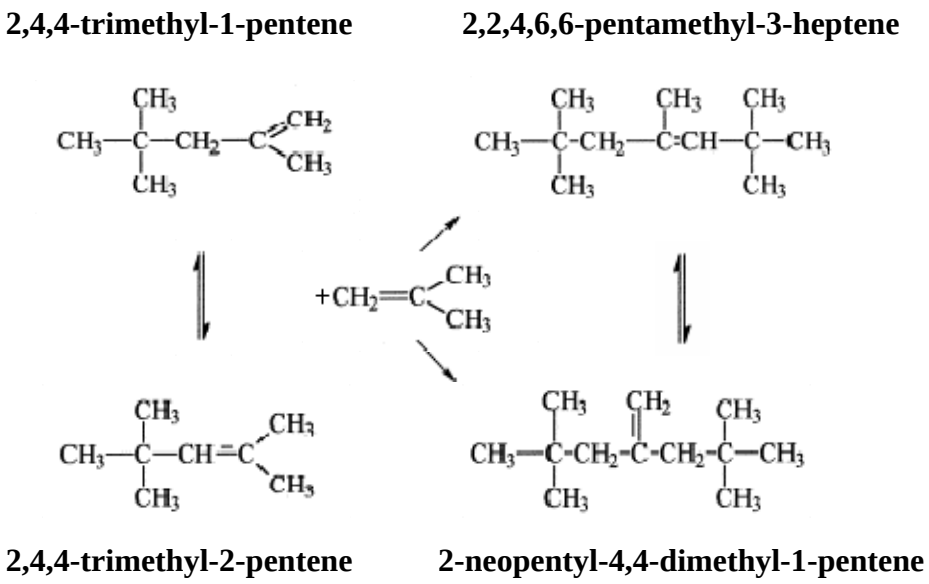

Scheme 2. Triimerisation of 2-methylpropene

The net rates of formation for the different components (r_{IB}, r_{DIB}, and r_{TRIB}) can be calculated using the reaction rate for DIB formation in the dimerization reaction $r_{DIB,j}$

and the reaction rate for TRIB formation in the trimerisation reaction $r_{TRIB,j}$, where following mechanism is used to derive the rate equations. In this mechanism the net rates are

$$r_{IB} = -2r_{DIB} - r_{TRIB} \tag{3.1}$$

$$r_{DIB} = r_{DIB} - r_{TRIB} \tag{3.2}$$

$$r_{TRIB} = r_{TRIB} \tag{3.3}$$

The temperature dependence of the reaction rate constants is calculated with the Arrhenius equation

$$k_i = F_i \exp(-E_i/RT) \tag{3.4}$$

where F_i is the preexponential factor, E_i the activation energy of the reaction, and R the universal gas constant. This equation was reparameterised to the form

$$k_i = F_i \exp(-E_i/R(1/T - 1/T_{ref})) \tag{3.5}$$

where T_{ref} is the reference temperature and F_i and E_i are the parameters to be optimised. In the final model, T_{ref} is chosen to be 373.15 K and the adsorption equilibrium parameters are assumed to be independent of the temperature.

The kinetic models that were derived are presented in the following, and the parameters for the rate equations can be found in Table 3. Parameters B_i in the table 3 represent the ratio of the adsorption equilibrium constant of component *i* to that of IB.

Dimerization Rate Equations:

$$\begin{aligned} r_{DIB} &= \frac{k_{DIB} a_{IB}^2}{\left(a_{IB} + B_{TBA} a_{TBA}\right)^2} \\ k_{DIB} &= F_{ref,DIB} e^{-\frac{E_{DIB}}{R}\left(\frac{1}{T} - \frac{1}{T_{ref}}\right)}, T_{ref} = 373.15K \end{aligned} \tag{3.6}$$

Trimerization Rate Equation:

$$\begin{aligned} r_{TRIB} &= \frac{k_{TRIB} a_{IB} a_{TRIB}}{\left(a_{IB} + B_{TBA} a_{TBA}\right)^3} \\ k_{TRIB} &= F_{ref,TRIB} e^{-\frac{E_{TRIB}}{R}\left(\frac{1}{T} - \frac{1}{T_{ref}}\right)}, T_{ref} = 373.15K \end{aligned} \tag{3.7}$$

The rates given by equations 3.6 and 3.7, as well as the rate given for TBA decomposition in table 3, have to be multiplied with catalyst density in the reactor to obtain the reaction rates in mol/(s·m^3).

Honkela *et al.* (2004) studied the deactivation of the catalyst during their experiments. Although a minor increase in the IB flow and a decrease in the DIB flow were

observed at the end of the experiment, the change was so small that deactivation was not included in the kinetic models.

3.2. Decomposition of 2-methyl-2-propene

Both the dehydration of tert-butyl alcohol (TBA) to 2-methylpropene and the reverse reaction have been studied widely. TBA production is of interest because of the use of TBA as a gasoline component [RON (research octane number) = 109, MON (motor octane number) = 91]. TBA formed as a side product in 1,2-epoxypropane synthesis is used not only as a gasoline component but Abraham and Prescott (1992) used it also in the production of 2-methylpropene for methyl tert-butyl ether (MTBE) and Morse (1999) for the production of other high-octane gasoline components. Also, direct routes from TBA to ethers (without 2-methylpropene formation in between) have been published by Matouq and Goto (1993), Yin *et al.* (1995) and Assabumrungrat *et al.* (2002).

The hydration of 2-methylpropene on ion-exchange resins is different from the dehydration of TBA because a large amount of water is present in the catalyst. Gupta and Douglas (1967), for example, carried out experiments in which water was present in large excess so that the resin was fully swollen. They obtained first-order irreversible kinetics for the hydration reaction.

Delion *et al.* (1986) applied various solvents in the hydration of 2-methylpropene with the aim of keeping the mixture in a single liquid phase. They tested p-dioxane, acetone, nitromethane, butylcellosolve (2-butoxyethanol), isopropyl alcohol, cyclohexanol, tetrahydrofurfurylic alcohol, and acetic acid and calculated solvent-dependent equilibrium constants for the reaction. Velo *et al.* (1990) obtained both equilibrium constants and kinetics for the hydration of 2-methylpropene. The kinetic equations were based on a carbonium cation mechanism in which 2-methylpropene forms a tert-butyl cation with the proton of the catalyst. They also concluded that TBA inhibits the hydration of 2-methylpropene more than water.

Diffusion has also been studied in other publications. TBA dehydration studies by Gates *et al.* (1972) and Heath and Gates (1972) indicate that, when macroporous ion-exchange resins are used as catalysts, mass-transport limitations do not exist.

The equilibrium reaction between TBA and water + 2-methylpropene is shown in scheme 3.

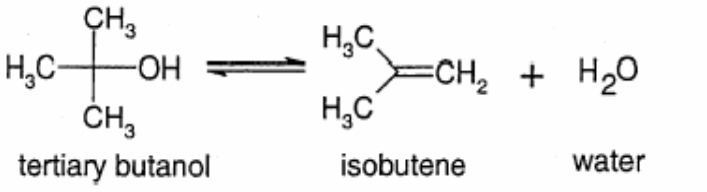

Scheme 3. Equilibrium between tert-butyl alcohol and water and 2-methylpropene.

The parameters of the kinetic models were determined using Kinfit software with the Levenberg-Marquardt optimization algorithm. In the optimization, various kinetic models were combined with an ideal batch reactor model, and the calculated compositions were compared with the measured ones.

The temperature dependence of the rate constants was described by the Arrhenius equation

$$k_i = F_i \exp(-E_i/RT) \tag{3.8}$$

where F_i is the preexponential factor, E_i is the activation energy, and R is the universal gas constant. This equation was reparametrized to the form

$$k_i = F_i \exp(-E_i/R(1/T - 1/T_{ref})) \tag{3.9}$$

where T_{ref} is the reference temperature and F_i and E_i are the parameters to be optimized. T_{ref} was chosen to be 343 K (70 °C). The adsorption equilibrium parameters were assumed to be independent of temperature.

In the tested models, the reaction on the surface of the catalyst was considered as the rate-determining step, and the active sites of the catalyst were assumed to be equivalent. Parameters for a model that took into account the different active sites that result from alcohol adsorption were determined, but they did not give satisfactory results.

Furthermore, adsorbed components were assumed to occupy one surface site, and the reaction was assumed to proceed through carbonium ions. Because very low adsorption equilibrium constants ($<1 \times 10^{-8}$) were obtained for isopentane in preliminary kinetic modeling, adsorption of the nonpolar components, i.e., isopentane and isooctane, was not included in the models.

The reaction equilibrium constant K_a determined experimentally was used in the models. The models are presented in the following subsections, and the rate equations for the dehydration of TBA can be found in Table 3. The rates for the other components in the dehydration of TBA follow the equation

$$r_{IB} = r_{H2O} = - r_{TBA} \tag{3.10}$$

Water is more polar than 2-methylpropene, which means that it adsorbs preferentially on the active sites. In this model, the formed 2-methylpropene does not adsorb on the catalyst, and only one active site is needed. Thus, the model follows a Langmuir-Hinshelwood-type mechanism with one active site. It was assumed that there are no unoccupied active sites on the catalyst. The model in which some of the active sites were unoccupied was tested, and it resulted in very similar parameter values. For the model, three parameters have to be determined: two parameters for the rate constant and the ratio of adsorption equilibrium constants of water and TBA.

Table 3. Kinetic equations for dimerisation and trimerisation of 2-methyl propene, and TBA decomposition along with their parameter values.

Reaction		
1 Dimerisation of isobutylene	$r_{DIB} = \frac{k_{DIB} a_{IB}^2}{\left(a_{IB} + B_{TBA} a_{TBA}\right)^2}$ $k_{DIB} = F_{ref,DIB} e^{-\frac{E_{DIB}}{R}\left(\frac{1}{T} - \frac{1}{T_{ref}}\right)}, T_{ref} = 373.15K$	
2 Trimerisation of isobutylene	$r_{TRIB} = \frac{k_{TRIB} a_{IB} a_{TRIB}}{\left(a_{IB} + B_{TBA} a_{TBA}\right)^3}$ $k_{TRIB} = F_{ref,TRIB} e^{-\frac{E_{TRIB}}{R}\left(\frac{1}{T} - \frac{1}{T_{ref}}\right)}, T_{ref} = 373.15K$	
3 Tert-butyl alcohol decomposition	$r_{TBA} = \frac{k_{TBA}\left(a_{IB} a_{H2O} - K_a a_{TBA}\right)}{a_{TBA} + K_{H2O} a_{H2O}}$ $k_{TBA} = F_{ref,TBA} e^{-\frac{E_{TBA}}{R}\left(\frac{1}{T} - \frac{1}{T_{ref}}\right)}, T_{ref} = 343.15K$ $\ln K_a = -3111.9 \frac{1}{T/K} + 7.6391$	
Reaction	**Parameter**	**Value (Honkela *et al.*)**
1	$\mathbf{F_{ref,DIB}}$	**0.82**
	$\mathbf{E_{DIB}}$	**30**
2	$\mathbf{F_{ref,TRIB}}$	**0.065**
	$\mathbf{E_{TRIB}}$	**1.8**
1+2	$\mathbf{B_{TBA}}$	**7.0**
3	$\mathbf{F_{ref,TBA}}$	**0.21**
	$\mathbf{E_{TBA}}$	**18**
	$\mathbf{B_{H2O}}$	**1.5**

4 MINIPLANT

A miniplant was constructed at Helsinki University of Technology (HUT) between years 2000 and 2001. The purpose of the miniplant was to

- Speed up the design of new processes and process configurations,
- Test control and operation of individual process units and

– Contribute to design and verification of thermophysical models.

The main units of the miniplant are two distillation columns and four tubular reactors, supplemented with necessary accessories such as pipelines, vessels, pumps and automation. All equipment are coupled with quick connectors in order to be easily replaced when necessary. The feed flow rate is limited by pump capacity, which for a single pump varies between 0.15 kg/h and 0.5 kg/h. The temperature range is from – 30 °C up to 200 °C and the equipment is pressure tested up to 25 bar. The hardware details of the HUT miniplant are further discussed by Lievo *et al.* (2002).

The first task of the miniplant was to imitate Fortum Oy's NExOCTANE process for dimerising 2-methyl propene.

4.1. Reactors

The reactor system of the miniplant consists of fixed bed tubular reactors. The length of each tubular reactor is 1.3 m, constructed of SS-316L and designed for operating at pressures below 2.5 MPa and temperatures below 473 K. The internal diameter of the reactor is 16 mm having a concentric tube with a 6 mm outside diameter for placement of temperature measurement probes. Four temperature probes can be placed in each reactor. The position of the temperature probes can be changed in order to obtain the temperature profile over the whole length of the reactor. The estimated uncertainty for temperature measurements is ± 0.1 K and for pressure measurements ± 0.05 bar.

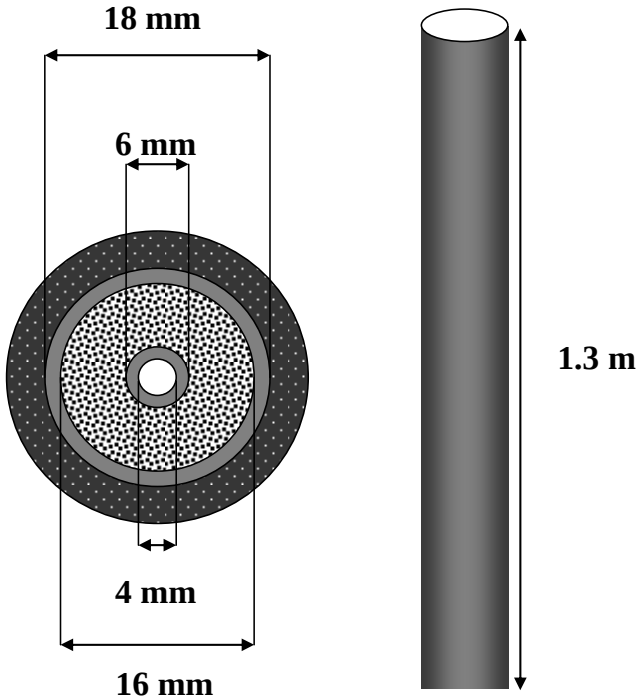

Figure 4. Schematic drawing of miniplant reactor. On the left, a cross-sectional drawing represents the layers from outside to inside: heating jacket, reactor wall, catalyst bed and thermowell.

The heating of the reactor is controlled by an external annular oil heating jacket, connected to a heating / cooling bath. The flow direction and flow rate of the heating fluid (technical white oil) are adjustable.

The reactors are in upright position, and the flow direction can be either downwards or upwards. The inlet section of the reactor can be packed with stainless steel springs to use it as heating section. This way the temperature of the fluid entering the catalyst section can be controlled; otherwise the feed mixture would be in ambient temperature due to cooling in the pipelines. The mass flow rates are measured by weighing type the feed bottles.

Figure 4. shows a schematic representation of the miniplant reactors.

4.1.1. Derivation of mathematical model

Tubular catalytic reactor models can be categorised based on number of dimensions and phases considered in the modelling work. If radial temperature, concentration or flow profiles do not exist or are not of interest, the reactor can be modelled as 1-dimensional plug flow reactor. When external cooling or heating induces radial profiles in the reactor, a more rigorous 2-dimensional approach is required.

Mass transfer between the reactor fluid and the solid catalyst surface may play an important role in determining the local reaction rates inside a catalytic reactor. In this case, heterogeneous treatment, which models the solid and fluid phases separately, may be adopted. If the concentrations of the reactive components in the reactor are the same at catalyst surface and in the fluid due to rapid mass transfer, the system can be simplified and considered to consist of a single, pseudohomogeneous phase. The solid catalyst then has a role of a packed bed, hindering and mixing the flow of the fluid.

In our reactor system, external cooling and heating cause radial gradients inside the reactors. Therefore it is important to use a 2-dimensional model. In dimerisation of 2-methylpropene on solid ion exchange resin catalyst, according to the results of Honkela *et al*. (2004), heterogeneous treatment taking interphase mass transfer between fluid and catalyst into account is not necessary. Honkela *et al.* made their experiments in a CSTR-reactor, where the fluid can be assumed perfectly mixed. This is not the case for the tubular reactor, where the fluid flow is laminar and mixing occurs by fluid flow through the catalyst bed. However, in strongly laminar flow conditions, the effect of stagnant film around particle surfaces disappears (as discussed later) and mass transfer between the fluid and catalyst surface is thus not markedly prohibited. Therefore pseudohomogeneous approach is adequate for treating the catalyst bed.

Another important topic to be addressed is whether radial and axial dispersion should be taken into account. Legaview and Ziolkowski (1995) state that if l_R/d_R – ratio is more than 50, axial dispersion effects become negligible. Here that l_R/d_R – ratio is around 100, so axial dispersion is not included in the set of equations.

Radial dispersion is mainly caused by turbulent effects. Here the flow is strongly laminar ($5 < \mathrm{Re}_p < 20$), so radial dispersion is partially neglected, and only diffusion and mixing due to the catalyst bed are included in the model equations.

The bed porosity closer to the walls is higher than in the middle of the catalyst section. At the point where the catalyst pellets meet the wall, the porosity is 1, and the flow is thus higher in regions close to the walls. This phenomenon is called channelling and bypassing, studied e.g. by Schwartz and Smith (1953), Calderbank and Pogorski (1957), Schlünder (1977) and Martin (1978). Here the catalyst section is annular, and the flow will therefore be channelled to the vicinity of both inner and outer tube walls. The porosity profile after Winterberg and Tsotsas (2000) for annular geometry is as follows:

$$\varepsilon = \varepsilon_{ave}\left(1+1.36e^{\frac{-5(R_o-R)}{d_P}}\right) \quad ,R \geq \frac{R_o}{2}$$
$$\varepsilon = \varepsilon_{ave}\left(1+1.36e^{\frac{-5(R-R_o)}{d_P}}\right) \quad ,R < \frac{R_o}{2} \tag{4.1}$$

Where ε_{ave} is the average porosity of the bed and R_o the radius of the reactor tube. R in eq. 4.1 is taken to be in the middle of the discretized layer.

Axial conductance of the reactor outer wall is neglected and it is assumed to be at the same temperature as the heating coil fluid. This assumption is justified since the overall heat transfer resistance between the heating fluid and the reactor wall is negligible, due to the high flow rate of the heating fluid.

Landon (1996) studied the effects of a concentric axial thermowell in a tubular reactor. He made calculations in various conditions including sharp temperature gradients, and concluded that the temperature difference between the surrounding fluid and the thermowell did not exceed 0.8 K at any circumstances. Therefore the thermowell temperature is assumed to be the same as that of the surrounding fluid in our calculations. The effect of the thermowell is then shown only in the tunnelling of the fluid in the vicinity of the thermowell wall.

The temperature for the counter-currently flowing heating fluid (T_{heat}) is calculated from equation 4.2,

$$\frac{\partial T_{heat}}{\partial z} = -\frac{\alpha_{hw}\pi d_{ext}}{\dot{m}_{heat}c_{P,heat}}(T_{heat}-T_{wall}) \tag{4.2}$$

where α_{hw}, d_{ext}, $\dot{m}_{heat}$ and $c_{P.heat}$ are the heat transfer coefficient between the heating fluid and the reactor wall, the external diameter of the reactor tube, the heating fluid mass flow rate and the heating fluid heat capacity, respectively. The initial condition for eq. 4.2 is

$$(T_{heat})_{z=0} = T_{heat,0} \tag{4.3}$$

Since the pseudohomogeneous reactor volume is discretized in radial dimension, and the ODE solvers tend to discretize the length of the reactor as well, the reactor volume is solution-wise divided in cells, where mass and heat transfer occurs with binary interaction between neighbouring cells. Naturally, at cells next-to-wall, no mass

transfer comes from the wall. Chemical reactions produce and consume components in individual cells, thus producing or consuming heat.

Radial heat transfer is described by the effective radial heat conductivity, λ_{er}, and the wall heat transfer coefficient, α_w. Radial mixing between the layers is caused by flow through the catalyst bed and diffusion of the components. In terms of mass transfer, radial mixing is modelled using the effective radial diffusivity D_{er}.

Dekhtyar *et al.* (2002) studied the heat transfer in packed beds at low Reynolds number with liquid phase flow. For wall heat transfer coefficient, they state that at inertial flow mode ($Re_p < 80$), the effect of the heat transfer resistance of the stagnant flow layer close to the walls becomes negligible. Calculating film thicknesses for these flow layers reveal that the thicknesses become so large that the entire reaction fluid can be considered to be within the film. The wall heat transfer coefficient α_w is generally used to describe this wall zone resistance, and in the absence of that resistance, a large value can be assigned for α_w and only λ_{er} is then used to describe the heat transfer inside the catalyst bed. The layers next to the wall are assumed to have the same temperature than the wall. This is important for the case in this study, since discretisation of the radial dimension conflicts with the use of α_w / λ_{er} –model, which also is not applicable with local bed porosities.

Several empirical correlations for λ_{er} for low Reynolds numbers and liquid phase reaction mixture were found from the literature (Dixon and Cresswell (1979), Agnew and Potter (1970) Bauer (1977) and Stankiewicz (1989). None of these correlations was fitted for systems with a particle Reynolds numbers below 20, so a more fundamental approach for λ_{er} was used. λ_{er} consists of static part λ_{er}^{0} and dynamic part λ_{er}^{t}.

$$\lambda_{er} = \lambda_{er}^{0} + \lambda_{er}^{t} \tag{4.4}$$

Static contribution can be approximated as a volume average from fluid and catalyst conductivities

$$\frac{1}{\lambda_{er}^{0}} = \frac{1}{\lambda_g} + \frac{1}{\lambda_{cat}} \tag{4.5}$$

where λ_g and λ_{cat} are the fluid and catalyst thermal conductivities, respectively.

The dynamic part of the term is based on effective axial diffusion caused by turbulence and flow through catalyst bed

$$\lambda_{er}^{t}/\lambda_g = aPrRe = a\rho_g v d_p/c_p \tag{4.6}$$

Zehner and Schlünder (1970) propose an expression for term a in (4.6) of form

$$a = \frac{0.14}{1 + 46\left(\frac{d_p}{d_o}\right)^2}, \tag{4.7}$$

but their experiments were made with gaseous fluid. Dekhtyar *et al.* (2002) state that a value of 0.1 can be used for a in most conditions with an error margin of ± 20 %. That value is used here

λ_{er} was calculated individually for each layer, and average values were used for heat transfer between two layers.

The dynamic part of the radial diffusivity of the bed, D_{er}, was calculated based on the analogy between heat and mass transfer, according to the following relation by Dixon and Labua (1985):

$$\lambda_{er}{}^{t} = \varepsilon \rho_g c_p D_{er} \tag{4.8}$$

where ρ_g is the fluid density and c_P the heat capacity of the fluid. Local averaged values were used for D_{er}. In the absence of turbulence, the effects of radial diffusion are negligible. The static part of the effective radial diffusivity is molecular diffusion. At these conditions, diffusion coefficients are of magnitude 10^{-4} in comparison to the dynamic radial diffusivity. They can therefore be safely neglected and are not included in this model.

Calculating the mass and heat balances for each individual annulus-shaped layer results in a set of ordinary differential equations. The equation system consists of enthalpy flow balances for each layer i (1…n) (equations 4.9-4.12), material balances for each component j (1…n_C) in each layer (4.13-4.16), and equations for heating fluid temperature (4.2 and 4.3).

The pressure drop in the reactor is approximated to zero, this assumption is based on low velocity of the fluid. The axial velocity profile varies only with the molar volume of the hydrocarbon mixture and as a function of the bed porosity ε.

The enthalpy flow $\dot{H}$ is the integrated variable instead of temperature T in the heat balances, and the heats of reaction are not included in the thermal balances as source terms. By calculating the enthalpy of the reaction mixture at each integrator step the heats of reaction, often temperature-dependent and inaccurate, can be neglected.

Heat is transferred to the catalyst bed only by conduction from adjacent layers of catalyst and by convection from inner and outer walls. The enthalpy balances for the layer next to the thermowell, here numbered as the first layer with subscript 1, have form of

$$\frac{d\dot{H}_1}{dz} = \pi\varepsilon\left(\alpha_w d_o \left(T_w - T_1\right) + \lambda_{er} d_2 \left(T_2 - T_1\right) \frac{n}{d_i - d_o} \right), \tag{4.9}$$

where α_w, λ_{er} and d_i and d_o are the wall heat transfer coefficient, the effective radial thermal conductivity and the inner and outer catalyst bed diameters, respectively. The enthalpy balance for the layer next to the tube outer wall is

$$\frac{d\dot{H}_{n(\max)}}{dz} = \pi\varepsilon\left(\alpha_w d_i \left(T_w - T_{n)}\right) + \lambda_{er} d_2 \left(T_{n-1} - T_n\right) \frac{n}{d_i - d_o} \right), \tag{4.10}$$

and for intermediate layers

$$\frac{d\dot{H}_i}{dz} = \frac{\pi\varepsilon\lambda_{er}n}{d_i - d_o}\left(d_n\left(T_{i-1} - T_i\right) - d_{i+1}\left(T_{i+1} - T_i\right)\right). \tag{4.11}$$

The enthalpy balances have initial condition for layer *i*

$$\left(\dot{H}_i\right)_{z=0} = \dot{H}_{i,0} \tag{4.12}$$

In the material balances for each component *j* (1…n_c) in each layer (4.13-4.16), the differential terms consist of mass transfer by diffusion between adjacent catalyst layers, and reaction term. The material balances for the layer next to the thermowell have form of

$$\frac{d\dot{n}_{1,j}}{dz} = \frac{D_{er}\varepsilon\pi d_2 n}{d_i - d_o}\left(C_2 - C_1\right) - r_j\rho_B\frac{\pi}{4}\varepsilon\left(d_2 - d_i\right)^2, \tag{4.13}$$

where $\dot{n}_{i,j}$, D_{er}, C_j, r_j and ρ_B are the molar flow of component *j* in layer *i*, the effective radial diffusivity, the concentration of component *j*, the reaction rate of component *j* and the bulk density of the fluid, respectively. The remaining material balances are

$$\frac{d\dot{n}_{n,j}}{dz} = \frac{D_{er}\varepsilon\pi d_i n}{d_i - d_o}\left(C_{n-1,j} - C_{n,j}\right) - r_j\rho_B\frac{\pi}{4}\varepsilon\left(d_o - d_{n-1}\right)^2 \tag{4.14}$$

for the layer next to tube outer wall and

$$\frac{d\dot{n}_{i,j}}{dz} = \frac{D_{er}\varepsilon\pi n}{d_i - d_o}\left(d_i\left(C_{i-1} - C_i\right) + d_{i+1}\left(C_{i+1,j} - C_{i,j}\right)\right) - r_j\rho_B\frac{\pi}{4}\varepsilon\left(d_i - d_{i-1}\right)^2 \tag{4.15}$$

for the intermediate layers. The material balances have initial condition for layer *i* and component *j*

$$(C_{i,j})_{z=0} = C_{i,j,0} \tag{4.16}$$

4.1.2. Case study: Dimerisation of 2-methylpropene in a tubular catalytic miniplant-scale reactor

The dimerisation of 2-methylpropene was studied in the miniplant reactors. Table 4 lists the TBA concentrations in the feed and the heating coil temperatures for the test runs. Also measured 2-methylpropene conversions and selectivities into diisobutene are listed in table 4 for each test run. The concentration of TBA in the reactor feed plays an important role in 2-methylpropene oligomerisation. TBA decreases the reaction rate for all polymerisation reactions, and therefore the reaction system is more easily controlled and temperatures can be increased to gain higher conversions with better selectivity.

Temperature profiles inside the reactor thermowell were measured by moving four temperature probes gradually down the reactor axial length. Isobutene dimerisation

(with molar heat of reaction of $\Delta H_r = -82.9$ kJ/mol according to Marchionne *et al.* (2001) or $\Delta H_r = -107.2$ kJ/mol according to Alcantara *et al.* (2001)) is a highly exothermic reaction as is the trimerisation reaction ($\Delta H_r = -157.4$ kJ/mol according to Alcantara *et al.* (2001)), and the axial temperature rise may lead to reactor runaway in case of uncontrolled heat transfer. Both dimerisation and trimerisation reactions are rapid at the beginning of the reactor bed, and the coolant fluid is unable to keep the temperature profile flat. Over 25 K temperature rises were measured, yet in those experiments the reactor was operated very close to runaway conditions.

In the reactor model calculations, the level of radial discretization is a trade-off between accuracy of the model and calculation time. One rule of thumb is that the thickness of a discretized layer should at least be equal to the diameter of the catalyst particle. Here the average particle size was $d_{p,ave} = 0.8$ mm, therefore the maximum amount of discretized layers is 6, resulting from dividing the thickness of the bed in the annulus, 5 mm, by the average catalyst diameter. Simulations with different discretization levels support this rule of thumb; the quality of the model prediction is not markedly improved when the bed is divided into more than 6 radial layers.

Table 4. Feed concentrations and operating temperatures for test-runs (two reactors in series). The catalyst bed length was 0.431 m for Reactor 1 and 0.592 m for Reactor 2. Average flow rate for all experiments was 280 g/h.

Feed IB (wt-%)	**Feed TBA (wt-%)**	**Set temp (K)**	**IB conversion (%)**	**DIB selectivity (%)**
40.20	2.62	333.15	28.4	98.3
28.79	2.53	333.15	24.7	96.6
28.79	2.53	338.15	36.4	95.8
28.79	2.53	343.15	49.7	94.6
28.79	2.53	348.15	62.9	93.3
40.71	1.22	323.15	40.6	95.4
24.20	1.23	333.15	48.3	90.6
24.20	1.23	338.15	59.1	89.9
40.70	1.16	318.15	21.3	95.9
32.05	1.16	323.15	33.2	92.1
40.48	1.78	328.15	30.5	96.9
28.13	1.99	333.15	33.4	96.5
28.13	1.99	338.15	49.3	94.7
28.13	1.99	343.15	60.2	93.6
25.82	0.68	317.15	34.9	88.0
25.82	0.68	320.15	49.4	86.8
25.82	0.68	323.15	62.2	82.7

Measured 2-methylpropene and TBA conversions together with selectivities into diisobutene and maximum thermowell temperatures are plotted against corresponding simulated values in figures 5 a-d.

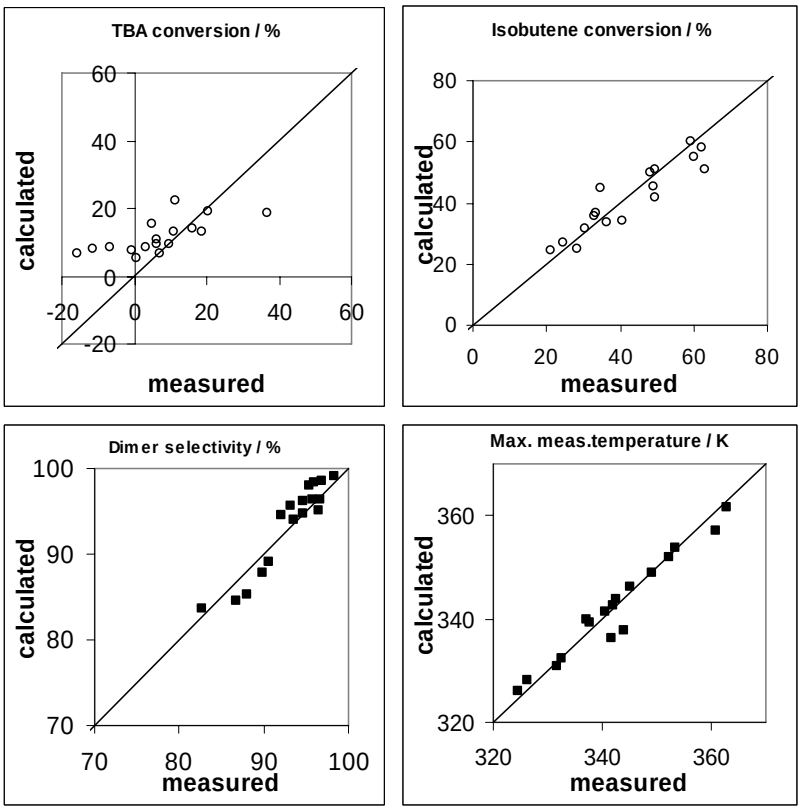

Figure 5. Comparison between measured and calculated TBA conversions (5a), 2-methylpropene conversions (5b), diisobutene selectivities (5c) and maximum bed temperatures (5d).

For both conversion and selectivities, the general trend of the simulated values seems to coincide well with the measured values. Predicted TBA conversions, however, seem to differ from measured values. Reasons for that might include mass transfer resistance and absorption and desorption of both TBA and water as polar components into and from the ion exchange resin. The effect of TBA decomposition on the dimerisation reaction is reduced by the fact that also water operates as a selectivity-improving agent.

Most of the models for calculating the radial thermal conductivity presented in the literature, empirical or semi-empirical, are based on the experimental results in a system with turbulent fluid and often with a gaseous reaction mixture. At high Reynolds number and turbulent conditions the dynamic term of equation 4.4 becomes dominant. Turbulence also improves radial mixing inside the reactor, and therefore turbulent conditions are usually preferred when operating such reactors. Here, however, the particle Reynolds number does not exceed 10 (20 in the vicinity of the wall boundary) in any of the test runs, so the flow is laminar. In equation 4.4, this results in equally significant dynamic and static term.

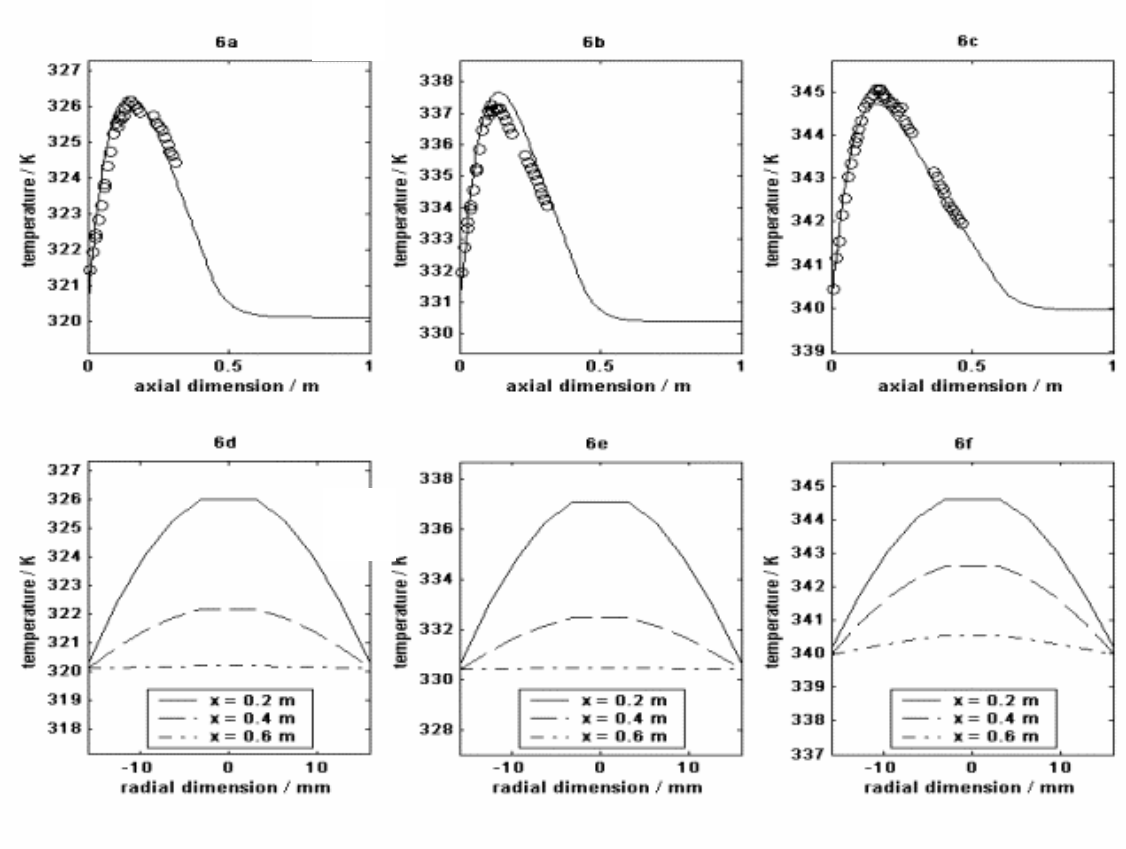

Figure 6. 6a-c(top); Axial temperature profiles of the catalyst bed; measured (o) and calculated (-) axial temperature; 6d-f (below); Radial temperature profiles at (-) x = 0.1 m ,(--) x = 0.2 m and (-.-) x = 0.3 m, x = position at the reactor axis measured from the beginning of the catalyst bed.

Figures 6a-c plots axial thermowell temperature profile inside the thermowell, and in figures 6d-f, radial temperature profiles are plotted at various points of the reactor axis. Both the maximum bed temperatures and axial locations of temperature maximums are accurately predicted. The average error in temperature maxima is 0.40 K.

Since heat is transferred by conductance, and no temperature jump occurs at the wall boundary layer, the radial temperature variations are as large as the axial ones. Therefore it can be concluded that 2-dimensional model is necessary for accurately predicting the reactor performance. Furthermore, dimerising 2-methylpropene in laminar flow region in an externally cooled tubular reactor can not be seen as an industrially interesting option, since due to poor radial conductivity, increasing the radius of the reactor would increase the risk of reaction runaway at the centre-regions of the tube and catalyst bed.

Possible causes for errors in the temperature profiles include thermal oil flow rate, errors in the inlet temperature of the fluid and analytical errors in the feed compositions etc. Taking these factors into account, the model performs the task of temperature profile prediction well.

Measured temperature rise in the entrance of the reactor is for some experiments sharper than the calculated one. Fluid maldistribution in the bed entrance may also be

one reason for slower calculated initial reaction rates. The catalyst shrinks when water and TBA is desorbed from it, and thus leaves an empty section at the top of the reactor tube. The flow channels in the vicinity of the walls, and has higher superficial velocity and hence better mixing at the near-wall regions of the bed. Therefore the heat is not transferred through the catalyst bed centre at the beginning of the bed. Here the superficial velocities are between 1 mm/s and 2 mm/s, so flow channelling is unlikely to occur in significant amount.

The experiments were modelled using a 2-dimensional tubular reactor model including equations for thermowell and external heat transfer to and from a heating jacket. At laminar flow regime, the thermal resistance of the wall layer becomes negligible, and hence only effective radial conductivity was used to describe the heat transfer in the catalyst bed. Temperature variations and peak locations inside bed were well described with this model.

The results in terms of conversion and selectivity of 2-methylpropene into diisobutene were rather accurate. Dynamic absorption of polar components in the catalyst resin was found to affect the measured TBA conversions to some extent, and the steady-state model could not predict the TBA conversions accurately for all test runs.

4.2. Distillation column

The distillation column of the miniplant ($\varnothing_{ID}$ = 39.4 mm) consists of compatible, 25 cm and 50 cm long packing units. The column is insulated with glass wool and aluminium foil, but still at temperatures higher than 100 C, the effect of the heat losses becomes important and some of the vapour condenses inside the column instead of making it way to the condenser.

The main packings are stainless steel springs (height = 4 mm, ∅= 4 mm). A 2 cm layer of Intalox saddles (height = 10 mm, width = 11 mm, ∅ = 6 mm) was used in the ends of the packing units between wire mesh (6mm) and springs to prevent the springs from penetrating through the mesh. The wire mesh may also at some conditions enhance the liquid distribution through the column cross-sectional area. There was a 2 cm long, empty space at the ends of all packing units. All packing units have two pockets for temperature measurement probes.

The reboiler is heated using an electrical heater with freely adjustable power (0…1 kW). Temperature and pressure ranges are 1…2.5 MPa and 0…250 ºC, respectively. Liquid level in reboiler is monitored visually.

The condenser used is a cross flow condenser, which is mounted to an angle of about 20 degrees so that the upper outlet connection is connected to the ventilation line and the lower one is connected to the reflux drum. The condenser is initially sized for large flow rates at high temperatures. Therefore it is difficult to set the flow rate of the cooling water so, that the condenser would operate as total condenser. Instead, it tends to subcool the reflux flow returned in the column. This causes condensation in the top section of the column, and must be taken in to account in simulations.

There is a possibility to use 14 temperature and two online pressure measurements inside the column. Flow rates in and out of the system are measured using scales,

since calibrating pumps for compressible hydrocarbons would result in less reliable mass balances. All data can be stored.

Liquid sampling can be done from the reboiler and from the reflux drum. There are four connections at the side of the column, from which vapour sampling is possible. However, the reliability of the vapour samples is questionable, since the sampling line must be purged with vapour before the sample is taken. For a sensitive distillation system, purging causes significant disturbances in the column composition profile and once the sample is taken; it may not represent the actual steady state. Liquid samples are drawn from a larger volume, from the reboiler and from the reflux drum, and therefore liquid sampling does not cause disturbances in the system, at least not in the same magnitude as with vapour samples.

4.2.1. Model for distillation

In our simulations, we used the modification of the Murphree multicomponent model for packed columns as presented by Keskinen *et al.* (2002).

To test the separation efficiency of miniplant column packings, a test-run was made with a mixture of n-hexane and cyclohexane. Also the heat losses and pressure drops were estimated from test-run results.

For the test-run, the column was built up as shown in Figure 7. The height of the packing section was 2 meters and there were 8 temperature measurements and two sampling points inside the packing section. Under the packing section all liquid was withdrawn out of the column and flow rate was measured with rotameter and returned back to the column through adjustable heating rod to compensate heat losses.

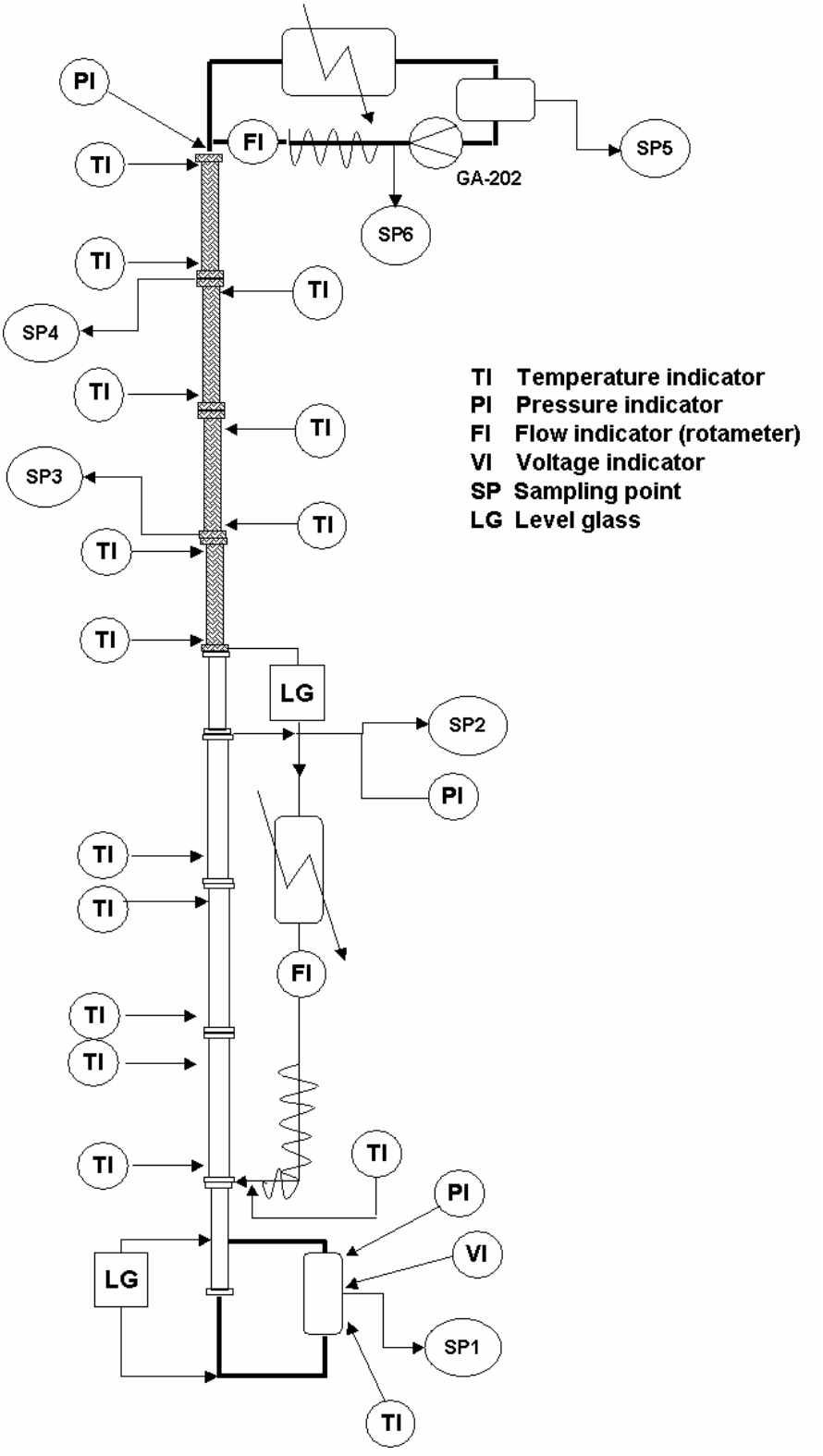

Figure 7. Experimental set-up for n-hexane – cyclohexane distillation test run.

The experimental plan consisted of several runs in different conditions using total reflux. The variables were pressure (ranging from 0.4 to 1.0 MPa), composition (25 % to 75 % for both n-hexane and cyclohexane mass percentages) and heating (150…500 W). The steady state was observed by following the temperature profiles, reflux pump

settings, pressure and rotameter values. When steady state was achieved, samples were taken from reboiler, condenser and packings section simultaneously and analysed using a gas chromatograph.

As no adequate correlation for calculating the mass transfer coefficients and areas for the springs were available we made a set of test runs to estimate the HETP of the packing. The column operated in total reflux, which means that after inserting the initial batch into the reboiler and the condenser, no feed streams were taken out of the column. The HETP was determined by simulating the column and by altering the number of ideal stages to match the simulated compositions with the measured ones. One ideal stage was included to represent the empty part of the column

Simulation of total reflux is not straightforward with a steady-state distillation model since it is designed to simulate distillation columns in usual operation modes. For simulation of the total reflux operation we chose the approach where the total reflux is simulated by feeding a large stream in the column reboiler and taking in practice only one product stream out of the column (from reboiler). The composition of the feed stream is the same as the measured reboiler composition; this way the simulated bottom composition matches with the measured one. The reboiler duty is also matched with the measured one to set the inner flows in the column equal to the real column. A small product stream is taken out from the top of the column, and the magnitude of the top product is decreased until the bottom composition shows no change to a further decrease in the top stream flow rate.

HETP was calculated and plotted as a function of f-factor. F-factor (vapor kinetic energy term) is calculated as a product of vapour superficial velocity v_t and square root of vapor density ρ_g, according to equation 4.17.

$$\frac{F}{\sqrt{kg/ms^2}} = \frac{v_t}{m/s} \cdot \frac{\sqrt{\rho_g}}{\sqrt{kg/m^3}} \tag{4.17}$$

The graph resulting from these calculations is shown in figure 8. Based on the results, the HETP value for the feasible operating range of the column is 0.055 m.

When operating such a small column special attention needs to be paid in calculating the heat losses. The heat losses were calculated for the condenser, reboiler and column body. The heat losses from the column body were calculated and distributed among the theoretical stages. Considering the column structure in figure 7 it was possible to calculate the heat losses with a reasonable degree of detail.

It is obvious that in such small equipment the reflux from the condenser was somewhat smaller than the measured liquid flow due to the heat losses. This has to be kept in mind when interpreting the HETP values of the packing presented in figure 8.

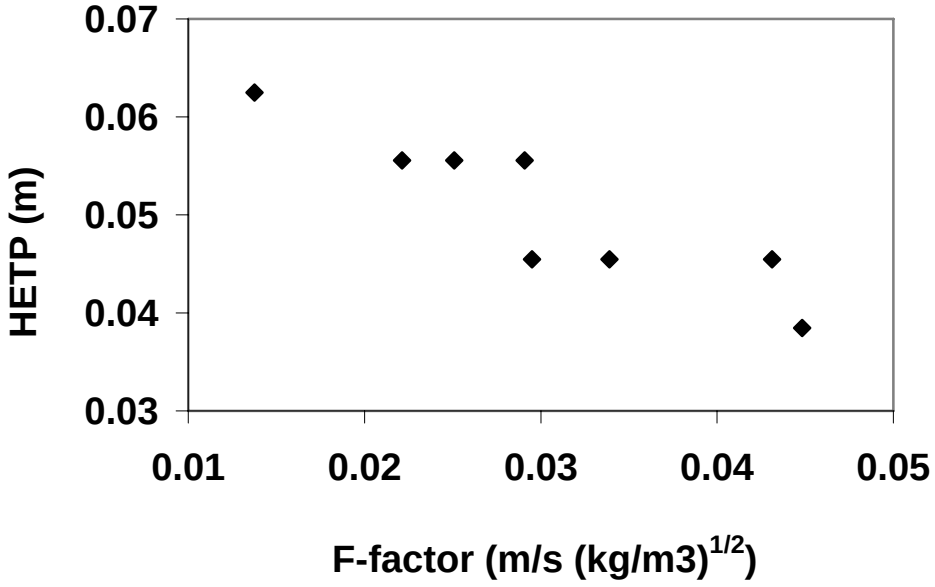

Figure 8. HETP values plotted against the vapor kinetic energy term (F-factor)

Pressure loss in the column did not exceed 0.01 bar at any of the test runs and therefore did not have a significant effect on the column behaviour or on the measured variables. Pressure loss was therefore neglected in the calculations.

4.2.2. Case study: Distillation of the dimerisation reaction mixture in a miniplant column

In order to test the VLE model for dimerisation reaction mixture, a rigorous model for miniplant distillation column was built. Modelling heat losses and HETP values for the column required a set of experiments that were done with a mixture of n-hexane and cyclohexane. The procedure for the model constructions is explained in section 6.2.

The column was then operated with the real reaction mixture coming out from the dimerisation reactors. The experimental set-up was made using a 2.5-meter high column with three product stream take-outs.

There were seven temperature indicators in the column and a voltage indicator in the reboiler. Frequent GC analyses were made for feed and output streams of the column. The pressure in the column was 0.9 MPa and the temperature range was 50…200 ºC.

The feed into the column comes from catalytic reactors, where 2-methylpropene is dimerised into isooctene. The feed consists mainly of isobutane, dimerisation products and unreacted 2-methylpropene. TBA is present only in small amounts, yet its presence affects the column behaviour markedly due to its non-ideal nature.

The column bottom product consists of diisobutene and heavier oligomers. A recycle stream back to the reactors is taken from the top part of the column. The recycle should contain as much of TBA and unreacted 2-methylpropene as feasible. Other light hydrocarbons fractionate between the top product and the recycle stream according to the separation efficiency of the top part of the column.

The main objective of the VLE model for the process is to predict the behavior of tert-butyl alcohol in a mixture of hydrocarbons. Of the components in the present mixture, TBA has azeotropes with water, diisobutene and isopentane. A prediction of these azeotropic compositions in the wide temperature range of the column is vital for a rigorous simulation. The temperature in the column varies roughly between 50 °C and 200 °C. The azeotropic composition in this temperature range predicted by our model and UNIFAC are compared to measured azeotropic compositions found from literature in figures 3a and 3b.

The column was simulated using all miniplant data available. The bottom product was set to contain only dimers and trimers, with the composition of other components not exceeding 0.01 w-%. The outtake from 32^{nd} stage, counted from reboiler up, was set to 100 g/h, which was the time-average of the real column outtake. Below the outtake the column stage number was calculated using the HETP values given in earlier. Above the outtake, the separation efficiency of the packing was greatly reduced by the fact that the condenser of the column did not operate as a total condenser, but also cooled down the temperature of the reflux flow below dew point. This was simulated by both reducing the number of theoretical stages and assigning heat losses to the stages above the outtake. According to the comparisons between simulations and miniplant data, this assumption was justified.

Since the composition of the bottom product was fixed, it was not included in the comparisons. Also the product flow rates were fixed, so this leaves the side-draw and top product compositions along with the column temperature profile as compared variables. Main emphasis in the simulation is laid on the key component compositions in the product streams. The key components are 2-methylpropene, TBA, and diisobutene. Other short-chained hydrocarbons function as indicators for column top section separation efficiency, but are not as vital for the operation of the column.

The column temperature profile is shown in figure 9 along with temperature probe locations. The column can be divided in three sections; at the bottom, the column is rich in diisobutene, in the middle section, TBA and C_4 hydrocarbons dominate and at the top part of the column the mixture consists almost entirely of light C_3 to C_4 hydrocarbons. With Wilson method, the dimer rich section reaches up to the 15^{th} –17^{th} stage. Dimer has high boiling temperature, and thus the temperature at dimer rich stages is close to 200 °C. In the middle section of the column, the effect of time-averaging the measured values produces some error. The horizontal fluctuation of the bell-shaped, TBA-rich composition profile causes the temperature to shift up and down. This also makes the column control difficult, and detailed knowledge about the column behaviour is vital for successful operation. The top section of the column, rich in C3 to C4 hydrocarbons, remains in rather steady temperature. The differences in the boiling points of short hydrocarbons are quite moderate, and therefore the changes in composition cannot be straightforwardly detected from the temperature profile.

TBA content is well predicted in both top product and side-draw. As a whole, the VLE-method, complemented with the column model, predicted the column behaviour successfully. The column model itself deserves credit for seemingly accurate HETP values. Both feed and product stream locations were placed strictly following the HETP calculations. Sub cooled reflux and heat losses cause the separation efficiency above the side-draw to be weak. This causes bad separation of C3-C4 hydrocarbons.

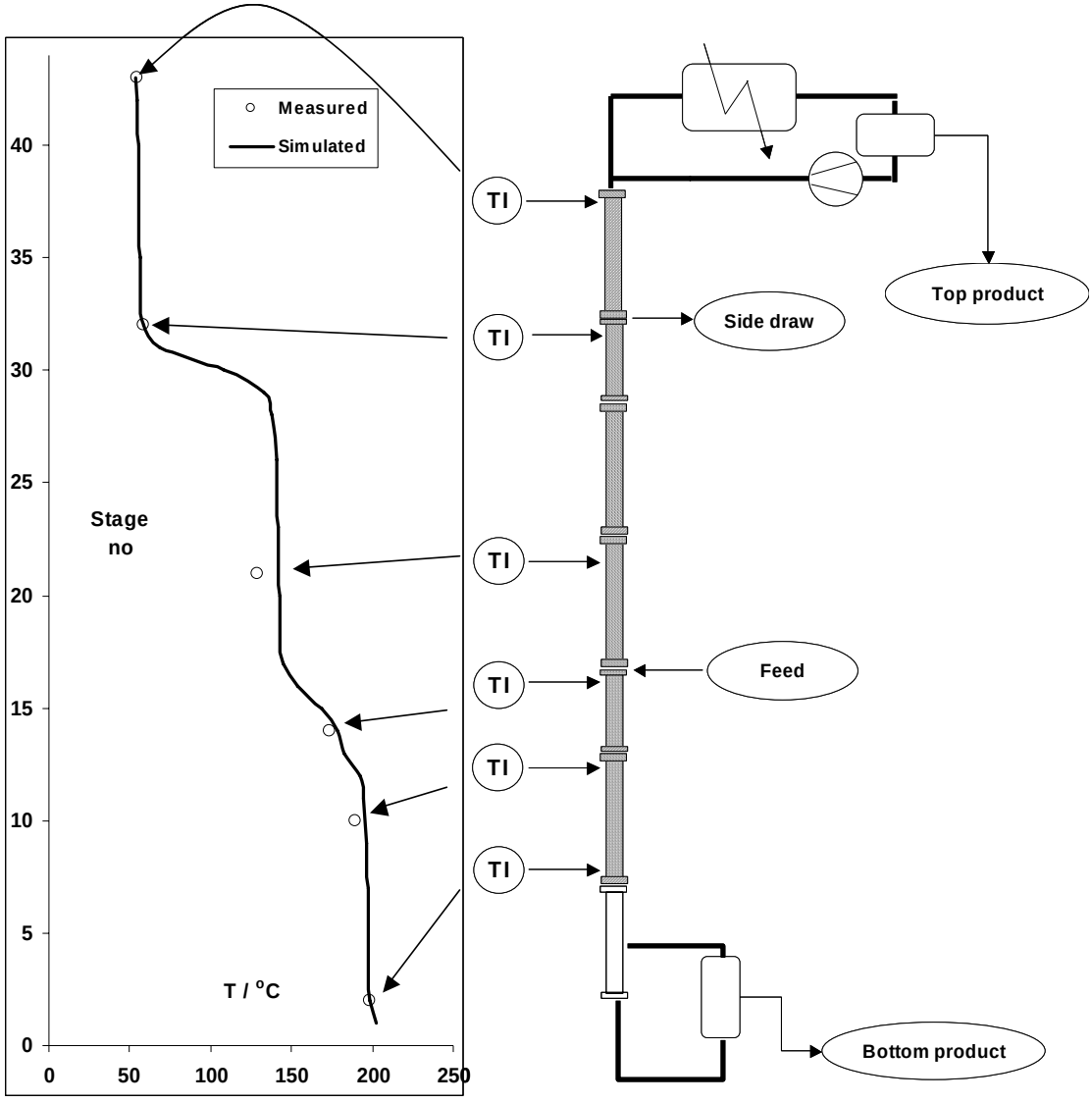

Figure 9. Column temperature profile. Circles present the measured temperatures and solid line the simulated profile. Temperature probe locations are connected to corresponding measured values with arrows.

The experience shows that miniplant concept can be successfully applied in process development. This study illustrates very well what is possible with the present modeling and analysis methods in distillation design. Nevertheless, miniplant concept can be further improved, in order to expand its possible applications.

Perhaps the most significant single improvement would be to build the miniplant equipment so that it can be operated unmanned at least overnight. Collecting, training and financing the operating staff is one of the main problems in performing a test run with a miniplant. If the purpose of the test is to verify the VLE model as in this case, it is enough to operate the column sufficiently long to certainly achieve the steady state and then perform the measurements. With a single distillation column this can usually be achieved in one or a couple of days.

However, when the goal is e.g. to check that there are no components accumulating to the system, longer runs are often necessary and this problem becomes acute. Unmanned operation has been reality with continuous reactors already a long time, but distillation columns have been too complicated devices to operate unattended.

Nevertheless, the small scale of a miniplant makes the unmanned operation thinkable. If the feed rate of the whole process is e.g. 0,2 dm^3/h, and product flow rates are of the same order, a feed tank of 20 dm^3 and product receivers of the same size are more than enough for operating the process over a weekend and the whole equipment may be sufficiently small to be built into a reactor bunker. When the diameters of the equipment are small, it can be designed to withstand high pressures giving a high safety margin.

On the other hand, small size causes problems. The system must be absolutely tight, because even a tiny leakage can ruin the material balance. Sampling may have effect similar to a leakage. Online analyzers connected so that only the amount strictly necessary is drawn from the process are to be preferred. As an additional problem, controllers suitable for small-scale equipment are often difficult to find.

5 SELECTION OF ENVIRONMENTALLY FRIENDLY PROCESSES

Increasing price of energy has led the chemical industry to consider the efficiency of their processes. Also the pressure from environmental legislation and worldwide trend for pollution prevention has forced manufacturers to reduce the amount of raw materials consumed in producing chemicals. Fortunately, in this case the environmental and economical benefits walk hand in hand, and as a consequence, during the last few decades, process integration and intensification have taken great leaps.

Combining separation and reaction in as single unit or unit block, such as in reactive distillation column, is often found beneficial in terms of chemical, utility and hardware costs. The separation part of the process can be simplified by pushing the conversion close to 100 % thus helping the separation of feed and product components. The idea is to increase the progress of equilibrium reactions by removing the products of the reaction continuously. High conversion in a single unit leads also to lower or negligible recycle streams. The heat of reaction can in case of exothermic reactions used for the separation.

The most studied and utilised combinatory process for reaction and separation is reactive distillation. In a reactive distillation column, the catalyst is placed inside the column so that the products are being constantly removed and the precursors are kept in the reactive zone of the column for increasing the conversion. Not all reaction systems are suitable for reactive distillation. The operation window of both reaction and separation must overlap in order for the process to be beneficial and efficient, the catalyst must be thermally stable and the selectivity of the reaction must be high enough at the temperature and pressure range of the column. A feasible solution must also be found for placing the catalyst inside the distillation column.

A reversible chemical reaction with unfavourable reaction equilibrium and with a significant heat of reaction may be a good candidate for a combined process. The most important application of reactive distillation today is production of ethers used

as gasoline enchanters. These fuel ethers are e.g. methyl *tert*-butyl ether (MTBE), ethyl *tert*-butyl ether (ETBE), *tert*-amyl methyl ether (TAME) and *tert*-amyl ethyl ether (TAEE). Esters have been produced using reactive distillation for decades, one of the first reports about RD esterification being that of Foerst (1955).

If a reaction is otherwise suitable for reactive distillation but it is slow, a large volume of catalyst needs to be placed inside the column. There is a contradiction between the requirements of having as much catalyst as possible in the RD column for the need of the reaction and at the same time of having a large void fraction to benefit the separation and enabling the counter-current two phase flow conditions. Taylor and Krishna (2000) and Pyhälahti (1996) have reviewed hardware structures of catalytic distillation. It is concluded that a large catalyst hold up is reached most probably by having the catalyst arranged in beds with vapour bypass and arrange the separation on every other stage by a normal distillation tray. The reactive stage is then actually kind of a catalytic tubular reactor without separation. If we add to this reasoning the catalyst deactivation, which is usually handled by adding an excess of catalyst to the reactor, we might conclude that the placement of the desired catalyst amount inside the RD column is in practice impossible for low reaction rates. Another typical way to compensate for catalyst deactivation is to raise the reactor temperature. This is at least difficult in a RD column. We agree with the reasoning of Althaus and Schoenmakers (2002) that considering RD in broader sense, disintegrating the reactor from the column is a most useful point of view.

In order to overcome the problems of RD and to maintain the benefits of the combined process, applying the side reactor concept (SRC) (Jakobsson *et al.* (2002)) or reactive pump around concept (RPA) (Althaus and Shoenmakers (2002), Baur and Krishna (2002)) can be considered. In SRC and RPA the flow is taken from the distillation column and introduced into a reactor or a series of reactors. In SRC the reactor or the reactor series is often temperature-controlled, or otherwise manipulated to reach optimal yield. Most often tubular reactors are applied. Reactor effluent is returned to the distillation column. The final product is then obtained from the distillation just as in RD processes. Compared to RD, adequate catalyst amount is more easily arranged in SRC and RPA where traditional reactor types and catalyst structures can often be used. Also the reaction conditions in SRC and RPA are less limited by the distillation requirements.

5.1. Process simulator

As the framework of the modelling we have used the sequential modular flowsheet program FLOWBAT. The program has features by which the user can define the calculation order of modules selected for the simulation. These have effect on the convergence of the overall process material balances. There are also several methods to be used for convergence acceleration.

FLOWBAT has several optimisation algorithms and in-house cost estimation capabilities for major equipments.

5.2. Reactive distillation model

Two types of reactive distillation models are available in our modelling tool. The first one is based on the equilibrium model (Kettunen, 1998) that was later expanded into

real plate model by including the calculation of plate efficiencies (Hyvärinen, 1998). In this model the reaction rate is taken into account as a source term in the mass balances. This is the standard way of taking the reaction into account in many commercial simulators. This is the case also in the second type of RD model, in our rate-based model but in that we have also included a model for fast reactions that take place in the liquid film by Kenig and Górak (1995) and a model for reaction and mass transfer in macroporous catalyst by Sundmacher and Hoffman (1996).

5.3. Side-reactor concept model

The available process simulation software tends to have problems in modelling all the relevant physical and chemical phenomena of the processes but often the problem lies in the convergence properties. Nonlinearities caused by e.g. thermodynamic functions, reaction kinetics and heat and mass transfer combined are a tricky combination to be solved even without recycle structure, not to mention with it. In case of reactive distillation solving the flowsheet is not an issue, since recycle streams are usually not present. Here, as well as often with SRC, the problem lies in the convergence of the distillation column. Multicomponent mixtures with azeotropes demand accurate models, and are rarely even close to linear.

One of the recent developments is a combined distillation side reactor model (Jakobsson *et al.* 2002). This combination is particularly interesting when new processes are developed since the interaction between the reactor and the distillation column is strong and tends to lead to convergence problems with traditional techniques. The unit block contains both the distillation column model and the models for the coupled reactors. To linearise the equations, tubular reactors are solved as series of CSTR's. This enables the model equations to be solved simultaneously in one block and not sequentially as it is done when the reactor/distillation systems are solved by traditional flowsheet programs. Fast convergence allows this unit model to be efficiently used in optimisation calculations.

5.4. Comparing SRC with RD

Comparison of the two process alternatives for combining reaction and distillation is here done in terms of industrial examples. The production of methyl acetate is a commonly seen example in demonstrating the applicability of RD. One might argue, however, that this particular process is not the best example to be used in general comparison between RD and other process alternatives, since it contains specific features that make it exceptionally suitable for RD. The azeotropes of the MeOAc production mixture make reactive distillation the most suitable combined process for MeOAc production (Agreda *et al.*, 1991). Furthermore, fairly easily separated products and the dependence of the reaction extent on the reaction temperature rather than the amount of catalyst favour reactive distillation as a process alternative for MeOAc production. Baur and Krishna (2002) made an important observation, however, showing that if each reactive stage in and RD column is replaced with a reactive pump around, the performance of an optimised RD column can be matched. This suggests that there is room for development in the field of optimising SRC or RPA configurations, and that performance of SRC's and RPA's should, at least theoretically, be superior to that of RD's.

5.4.1. Case study: TAME production

One commercially successful example of the application of SRC is the process for TAME production. In the process C5-tertiary olefins are converted to *tert*–Amyl–Methyl–Ether (TAME). Details of the process have been described by Jakkula, Järvelin & Kivi (1994), Koskinen, Järvelin & Lindqvist (1996), and Järvelin, Tamminen & Ewy (1996). Klemola (1996) has compares reactive distillation and side-reactor concept in TAME production using an economics-based objective in his study.

TAME is formed as a product of either 2-methyl-2-butene or 2-methyl-1-butene and methanol. The main reactions of producing TAME are as presented in scheme 4.

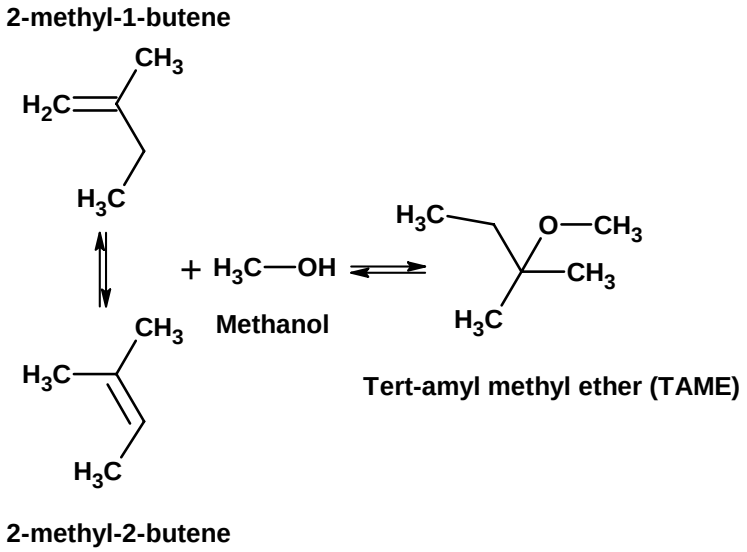

Scheme 4. Simultaneous etherification and isomerisation reactions involved in TAME synthesis.

TAME reaction is equilibrium limited (Rihko *et al*., 1994 and 1996) reaction where high conversion can be achieved only by combining multiple stage reactors with a separation system. The reaction rate increases with temperature, whereas at lower temperatures the reaction equilibrium is shifted towards the products. Combined reaction and separation allows sufficiently high reaction temperatures, since the product is being constantly removed and adjusting the temperature for more favourable equilibrium becomes less significant.

When applying reactive distillation to TAME production these benefits can be exploited to a certain extent. There are, however, a number of relatively heavy components at the reaction mixture, that force the distillation temperature to be fairly high. This leads to either a need for large catalyst amounts or alternatively to long residence times in the reactive stages of the column. The contradiction between the requirements of reaction and separation is well shown here. If either high catalyst amounts or large inner flows due to the demand for high residence times are applied to achieve feasible conversion, the reactive distillation column becomes very large. Applying side reactor concept in production of TAME does not necessarily remove the need for large catalyst amounts, but the catalyst can be better exploited when the single phase operating conditions are more freely adjustable.

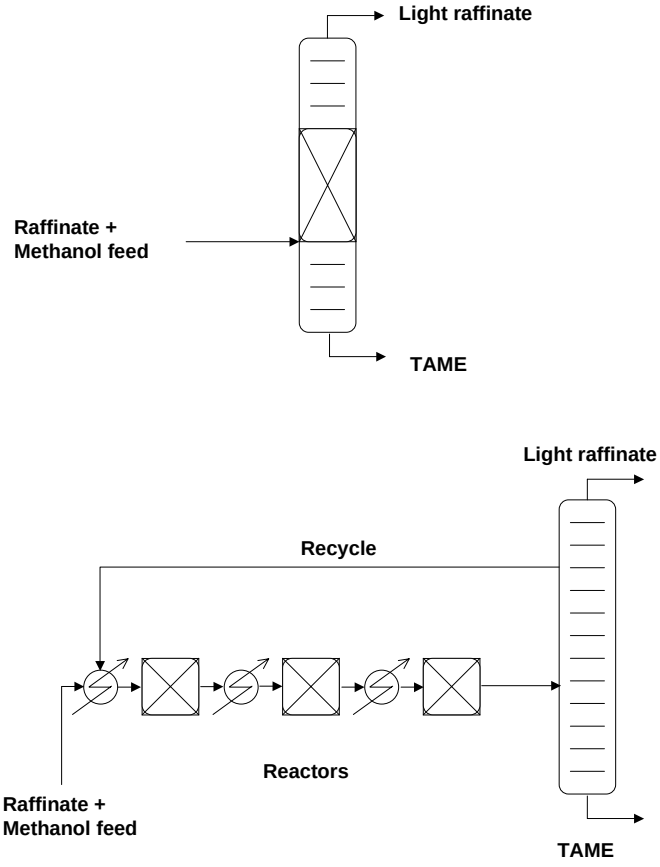

Figures 10a and 10b. Process configurations for producing TAME. Figure 10a (upper scheme) presents the reactive distillation column, and figure 10b (lower scheme) side reactor concept. In case of optimised side reactor concept, reactor feed temperatures are controlled by heat exchangers before the reactors.

TAME process was simulated with both RD and SRC. Process configurations are depicted in Figure 10a and 10b. In RD (Figure 10a), the column had a total of 30 ideal stages, of which 13 were reactive (stages 11-23). The amount of catalyst at one stage was set to be 800 kg, adding up to a total of 10400 kg dry catalyst in the entire column. Feed was introduced below the reactive zone, in order to prevent the light precursors from leaving the column with top product without meeting the catalyst

first. The column operated at a pressure of 5 bar, which set the reaction temperature to a feasible level (to around 343 K).

When SRC (Figure 10b) was applied, an amount of catalyst identical to RD-case (10400 kg) was divided between 3 reactors in series. First reactor contained 1160 kg, second 3490 kg and third 5750 kg of catalyst. The diameter of the column was 3.3 m for each of the reactors and lengths for 1st, 2nd and 3rd reactor were 1 m, 2 m and 6 m, respectively. The reactors operated at pressure of 15 bar, and without any external heating or cooling. The inlet temperatures were regulated in the case of optimised SRC. Distillation column with 30 ideal stages was used here as well. The feed from the 3rd reactor was introduced at stage 10, and the recycle stream back to the reactors was taken from stage 20. The column operated at pressure of 5 bar.

In Figure 11 the conversions of a reactive distillation system and two different side reactor configurations are plotted against reflux ratio of the system. In each configuration the catalyst amount is the same in the system. The feed composition is also the same for each configuration. The feed consisted of equimolar amounts of methanol and 2-methyl butene. It can be seen that the conversion in the reactive distillation column reaches its maximum value at relatively low reflux flow rates. Conversion in the adiabatic SRC (no heating or cooling between the reactors) rises steadily with the reflux ratio, reaching and surpassing the conversion of RD at high reflux ratios. The conversion of an adiabatic SRC stays below the one of RD's at lower reflux ratios, because part of the reflux flow is not going to the reactors, but is needed for the mass transfer purposes. Also the gas phase never meets the catalyst.

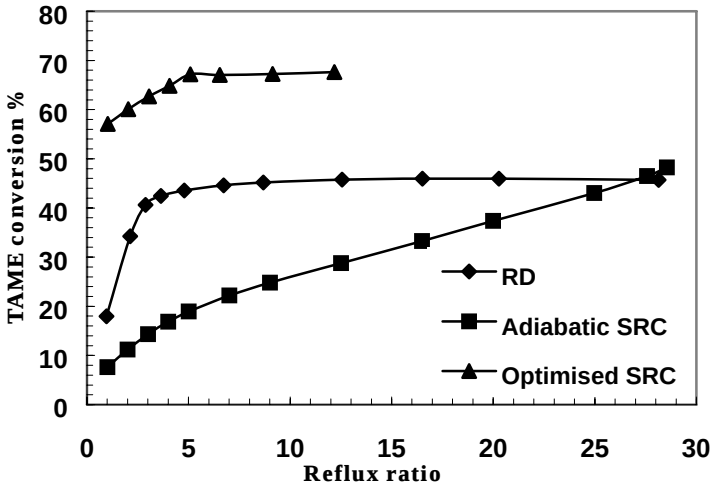

Figure 11. Comparison between conversions of reactive distillation, adiabatic side reactor concept and reactor train -optimised side reactor concept. TAME conversion is plotted against reflux ratio. For SRC the reflux flow rate is combined recycle and reflux flow rate.

When the inlet temperatures of the reactors are optimised, the results show a remarkable improvement in the conversion. Even with very low reflux ratios the conversion in the SRC exceeds the maximum obtainable conversion for RD. In case of TAME reaction the reason for increased conversion is clear. Since high temperatures favour high reaction rates, high conversion can be achieved in the first reactor with high inlet temperature and low catalyst amounts. Low temperatures and

high residence times can then be applied to the latter reactors, yielding a conversion higher than is possible to achieve with adiabatic reactor train.

The feed is introduced in to the reactor series when SRC is applied. Due to this, the conversion in SRC is at least the once-through conversion of the reactor series. In optimised case, the conversion of SRC at its minimum corresponds to the optimised once-through conversion of three tubular reactors in series. In adiabatic SRC, the once-through conversion is not so high, since all the potential of the reactor series has not been used.

Commercial TAME processes applying RD use a pre-reactor with a conversion of 65-70 % (Klemola, 1996). RD column feed then has a precursor/product ratio of around 1/3 in weight fractions. At these high conversion levels the superiority of SRC cannot be demonstrated as clearly as it is done for lower conversion levels. A number of simulations with a pre-reactor were performed in order to find optimal process conversions for SRC and RD. Both process alternatives could be optimised to give a conversion above 90 %.

At higher conversions, when a pre-reactor is applied, SRC loses part of it advantage. Since the output of the pre-reactor, which is the feed to the SRC, already has high conversion, it is not useful to introduce it to the reactor train. Hence the feed is introduced in the distillation column, and only the recycle stream from the column is led through the reactor train. However, more flexible reactor and catalyst options together with less restricted hardware design give SRC an upper hand. Therefore, as Klemola's study revealed, SRC is a better alternative in TAME producing when the objective is purely economical.

5.4.2. Case study: side reactor concept in dimerisation of 2-methylpropene

The dimerisation reaction of 2-methylpropene is a catalytic liquid-phase reaction, which sets requirements for the reactor pressure. Therefore the operating window for the reaction is fairly limited, which is known to be problematic from the reactive distillation point of view. When SRC is applied, the possibility of manipulating both the reaction and separation conditions is again significantly better.

The reaction is highly exothermic so it could still be an interesting candidate for reactive distillation. Hyvärinen (1999) investigated the possibilities of a RD process to produce diisobutene in industrially relevant scale. In the study the ideal stage reactive distillation model was used. The kinetic model is an in-house model. UNIFAC was used as the activity coefficient model. By trial and error some interesting designs was found of which some key figures are represented in table 5. These designs have 78 ideal stages. The feed is introduced on stage 7 (stage 1 is the reboiler). The combined dimer and the isooctane composition were kept under 0.7 mol-% in the simulations. Some of the designs included an external reactor.

The authors are fully aware that these designs are based on trial and error and are found through simulation with a preliminary model. Despite of this we believe that these results give useful ideas to consider. Designs A, B and D seem to be reasonable in respect that 300 kg of dry catalyst per ideal stage might be possible to implement in a RD column. However, the conversion of the 2-methylpropene is not high enough in designs A and D. Design B demonstrates the trend how the conversion can be

increased by a higher reflux ratio in this case 30.0. This value is obviously unrealistic, which can be seen from the reboiler duty 97.3 MW. Comparison of designs A and C shows how increasing the total amount of catalyst in the column affects the conversion. The conversion is significantly higher but the amount of catalyst reaches a value 1600 kg dry catalyst per ideal stage, this being unfortunately an unrealistic amount of catalyst per ideal stage.

Table 5. Column details, conversions and selectivities for 4 optimised reactive distillation columns for isobutylene dimerization

Design	**A**	**B**	**C**	**D**
Pressure in column [Mpa]	1.58	1.51	1.4	1.58
Reflux ratio	4.8	30.0	4.8	4.8
Reboiler duty [MW]	14.8	97.3	14.8	9.4
Catalytic stages in column	12-71	12-56	12-71	12-71
Dry catalyst on stage [kg]	300	300	1600	300
Dry catalyst in the column [kg]	18000	13500	96000	18000
Dry catalyst in the whole system [kg]	21475	16975	99475	18000
Conversion of isobutene in the column	91.2	95.3	95.3	93.0
Conversion of isobutene in the whole process	93.4	96.5	96.4	93.0
Dimer selectivity in column	88.2	94.2	86.0	89.3
Dimer selectivity in the whole process	90.9	95.3	89.2	89.3

A recent application to produce diisobutene with a side reactor process is proposed by Sloan, Brikhoff, Gilbert, Nurminen and Pyhälahti (2000). The isooctene product is taken from the bottom of the distillation column and the unreacted C4-stream is recycled into the reactor section. Side reactor concept does not place as strict restrictions on the amount of catalyst in the system as reactive distillation does. Optimising the inlet temperatures in the reactor train, and using one external reactor to push the overall conversion towards 100 % gives promising results even without any external heating or cooling. Optimising the feed temperatures of the reactors allows the overall conversion reach as high figure as over 99 %, keeping the selectivity at the same time over 95 %. The advantage of optimised SRC shows again in the fact that the selectivity can be increased at the cost of conversion, if desired, still keeping the overall yield at a higher level than is possible to reach with RD.

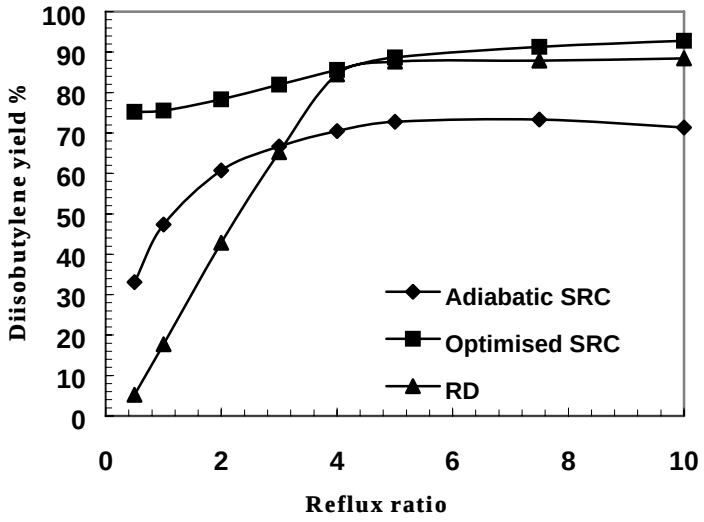

Figure 12. Comparison between conversions of reactive distillation, adiabatic side reactor concept and reactor train -optimised side reactor concept. Diisobutene yield is plotted against reflux ratio. For SRC the reflux flow rate is combined recycle and reflux flow rate.

Design A from Table 5 was picked as a reference process in comparing the performance of SRC in 2-methylpropene dimerisation. The results of the comparison are presented in Figure 12, where the overall yield of diisobutene is plotted against reflux ratio of the distillation column. The catalyst amount was 18000 kg dry catalyst in total in all simulations for RD and SRC. In case of adiabatic SRC the inlet stream to reactor train was at the same temperature as the column side-draw plate. In case of optimised SRC the inlet temperatures of the reactors in the reactor train were optimised.

The results are not as spectacular as in TAME production (Figure 11.), but it must be kept in mind that the even though heuristic, the optimisation of reactive distillation column was holistic, including feed compositions, number of ideal plates, pressure etc. Still the performance of the optimised SRC excels the one of RD at every reflux ratio. The performance curves of RD and optimised SRC overlap only at the vicinity of the optimal reflux ratio of RD, 4.8.

Adiabatic SRC does not in this case reach the performance of RD at high reflux ratio, but the quality of the product actually starts to decline at high reflux ratios. This is most probably due to the high flow rate through the reactors, which causes the temperature in the reactors raise less. This leads further to lower reaction rates.

The main reactions of both processes, TAME and dimerization, show characteristics that makes the process configuration combining closely distillation and reaction attractive. In both cases the side reactor configuration shows good techno-economical properties. The main advantage, according to the authors, of SRC over RD is the capability of having the full potential of both reactor and distillation units in use. This feature is highlighted at low conversion levels, as was shown in TAME example.

The contradiction between the large catalyst hold-up and high residence times required by the reaction and the large vapour space required by the distillation

diminishes the applicability of RD. There are additionally the well-known limitations of RD, like the narrow operating window and difficulties with the catalyst inside the column.

The results gained from both examples show, that side-reactor concept gives not only more freedom of choice in process design but is often a superior choice in terms of efficiency and economics. The full advantage of SRC is capitalized when the operating conditions in the reactor train are optimised.

6 CONCLUSION

Miniplant scale hardware with two distillation columns, 4 reactors and pumps and accessories was used in testing process conditions for dimerisation of 2-methylpropene. The experimental work included individual unit tests for the tubular catalytic reactors and distillation column, and VLE measurements as well as kinetic experiments for the reaction system of 2-methylpropene dimerisation.

VLE was measured for 2-methyl propane and 2-methylpropene at 313 K with C!-C4 alcohols. Model parameters for measured binaries were fitted for Wilson method and together with data from literature; a VLE model for the reaction system of dimerisation of 2-methylpropene was constructed. This model was compared with UNIFAC and verified against experimental distillation data. The results proved that together with an accurate distillation model the VLE model is sufficient for predicting the separation characteristics for the system studied.

Kinetic equations were derived for 2-methyl-2-propanol decomposition into water and 2-methylpropene. This model was combined with kinetic model for oligomerisation of 2-methylpropene. The models were tested against experimental data that was produced by running the miniplant reactors in different temperatures with different feed composition and measuring the product composition and temperature profiles of the reactors. The kinetic models, combined with a 2-dimensional pseudohomogeneous reactor model tailored for the miniplant reactors, gave an accurate description of what occurs inside the reactor during the experiments.

Both the hardware and thermophysical models developed in this work can be used separately, they are not interdependent. The thermophysical models are directly applicable to industrial scale and the hardware models can be used for other chemical systems as such. This is the ideology behind miniplant, developing and testing models that are not bound to each other and can be used in other conditions and for other scales.

Finally, a comparison between two reactive separation process alternatives was done. In addition to the dimerisation of 2-methylpropene, TAME production was used as an example system. The study revealed that even though reactive distillation is an efficient and intense process, side-reactor concept can be used to relieve the stringent limitations of reactive distillation. Side reactor concept was found an efficient method for producing both TAME and 2-methylpropene. Furthermore, side reactor concept combines reaction and distillation in an elegant fashion and gives an environmentally friendly, energy and raw material efficient and economically viable process alternative that is easily adjustable for the needs of today’s chemical industry.

REFERENCES

Abraham, O. C. and Prescott, G. F., Make Isobutylene from TBA, *Hydrocarbon Process.* **71** (1992) 51.

Agnew, J.B. and Potter, O.E., Heat transfer properties of packed tubes of small diameter. *Trans. Inst. Chem. Eng*. **48**, (1970) T15.

Agreda, H.V., Partin, L.R. and Heise, W.H., High-purity methyl acetate via reactive distillation, *Chem. Eng. Progress* **2** (1991) 40.

Alcantara, R., Alcantara, E., Canoira, L., Franco, M.-J., Herrera, M. and Navarro, A., Trimerization of isobutene over Amberlyst-15 catalyst, *React. Funct. Polym.* **45** (2000) 19.

Althaus, K. and Schoenmakers, H.G., Experience in Reactive Distillation, *International Conference on Distillation & Absorption,* Baden-Baden, Germany, 2002.

Assabumrungrat, S., Kiatkittipong, W., Sevitoon, N., Praserthdam, P. and Goto, S., Kinetics of Liquid-Phase Synthesis of Ethyl tert-Butyl Ether from tert-Butyl Alcohol and Ethanol Catalyzed by -Zeolite Supported on Monolith, *Int. J. Chem. Kinet*. **34** (2002) 292.

Baer, J. and Quitzsch, K., Mixed-phase thermodynamic investigations on the phase equilibrium behavior of ternary systems of the type C4-alcohol/water/diisobutene with a view to modeling a technologically feasible azeotropic dehydration procedure, *Wiss. Zeitschrift der Karl-Marx-Universität Leipzig. Ges.-wiss. Reihe*. **23** (1974) 621.

Barker, J.A., Determination of activity coefficients from total-pressure measurements, *Austral. J. Chem.* **6** (1953) 207.

Bauer, R., Effective radial thermal conductivity of gas-permeated packed beds containing particles of different shape and size distribution, *VDI-Forschungsheft* **582**, (1977) 39.

Baur, R. and Krishna R., Distillation column with reactive pump arounds: an alternative to reactive distillation, *International Conference on Distillation & Absorption,* Baden-Baden, Germany, 2002.

Calderbank, P.H. and Pogorski, L.A., Heat transfer in packed beds, *Trans. Instn. chem. Engrs.* **35** (1957) 195.

Davidon W.C., Optimally conditioned optimization algorithm without line searches. *Math. Progr.* **9 (**1975) 1.

Dekhtyar, R.A., Sikovsky, D.P., Gorine, A.V., and Mukhin, V.A., Heat Transfer in a Packed Bed at Moderate Values of the Reynolds Number, *High Temp.* **40** (2002) 693.

Delion, A., Torck, B. and Hellin, M., Equilibrium Constant for the Liquid-Phase Hydration of Isobutylene over Ion-Exchange Resin, *Ind.Eng.Chem.Process.Des Dev.* **25** (1986) 889.

Di Girolamo, M. and Marchionna, M. Acidic and Basic Ion Exchange Resins for Industrial Applications, *J. Mol. Catal. A:Chem.* **177** (2001) 33

Dixon, A. G. and Cresswell, D. L. Theoretical prediction of Effective Heat Transfer Parameters in Packed Beds, *AIChE J.* **25** (1979) 663.

Dixon, A.G. and Labua, L.A. Wall-to-fluid coefficients for fixed bed heat and mass transfer, *Int.J.Heat Mass Transfer* **28** (1985) 879.

Fischer, K., Park, S.-J. and Gmehling, J. Vapor-Liquid Equilibria for Binary Systems Containing Methanol or Ethanol, Tert-Butyl Methyl Ether or Tert-Amyl Methyl Ether, and Butane or 2-methylpropene at 363 K, *J. Phys.-Chem. Data* **2** (1996) 135.

Foerst, W. (editor), *Ullmanns Encyclopädie der Technishen Chemie*, 3rd edition Urban and Swarzenberg, Munich, 1955.

Gates, B. C., Wisnouskas, J. S. and Heath, H. W., Jr. The Dehydration of tert-Butyl Alcohol Catalyzed by Sulfonic Acid Resin, *J. Catal.* **24** (1972) 320.

Gmehling, J., Menke J., Krafczyk J. and Fischer K. *Azeotropic Data*, VCH, Weinheim, Germany, 1994.

Gupta, V. P. and Douglas, W. J. M. Diffusion and Chemical Reaction in Isobutylene Hydration within Cation Exchange Resin, *AIChE J.* **13** (1967) 883.

Heath, H. W., Jr. and Gates, B. C. Mass Transport and Reaction in Sulfonic Acid Resin Catalyst: The Dehydration of tert-Butyl Alcohol, *AIChE J.* **18** (1972) 321.

Honkela M.L. and Krause A.O.I., Influence of Polar Components in the Dimerization of Isobutene, *Catal. Lett.* **87** (2003) 113.

Honkela, M. L. and Krause, A. O. I. Kinetic Modeling of the Dimerization of Isobutene, *Ind. Eng. Chem. Res*. **43** (2004) 3251.

Honkela, M., Ouni, T. and Krause, O., Thermodynamics and kinetics of the dehydration of *tert*-butyl alcohol, *Ind. Eng. Chem. Res.* **43** (2004) 4060.

Hyvärinen, S., *Dimerointiprosessin prosessiteknisten Ominaisuuksien määrittäminen*, Master's Thesis, Helsinki University of Technology (In finnish), Helsinki 1998.

Ilme, J., *Estimating plate efficiencies in simulation of industrial scale distillation columns,* Ph.D. Dissertation, Lappeenranta University of Technology, Research papers 57, Lappeenranta 1997.

Jakkula, J., Järvelin, H. and Kivi, J., The Production of TAME and Heavier Ethers to Achieve Higher Oxygen and Lower Olefins Content in Motor Gasoline, New Fuels and Lubricants, Proceeding of *World Petroleum Congress*, Stavanger 1994.

Jakobsson, K., Pyhälahti, A., Pakkanen, S., Keskinen, K. and Aittamaa, J., Modelling of a side reactor configuration combining reaction and distillation, *Chem. Eng. Sci.* **57** (2002) 1521-1524.

Järvelin, H., Tamminen, E. and Ewy, G., NexTAME process operating experiences from a commercial unit and some economical considerations, *NPRA annual meeting*, San Antonio 1996.

Kawase, M., Suzuki, T. B., Inoue, K., Yoshimoto, K. and Hashimoto, K. Increased esterification conversion by application of the simulated moving-bed reactor, *Chem. Eng. Sci.* **51** (1996) 2971.

Kenig, E. and Gorak, A., (1995) A film model based approach for multicomponent separation process, *Chem. Eng. Proc.* **34** 97-104.

Keskinen, K.I., Kinnunen, A., Nyström, L. and Aittamaa, J., Efficient approximate method for packed column separation performance simulation, Proceedings of the *International Conference on Distillation & Absorption*, Baden-Baden, Germany, 2002.

Kettunen, M, Tislauksen mallitus kun reaktio tapahtuu kolonnissa, *M.Sc. thesis*, Helsinki University of Technology, Espoo 1998.

Klemola, K., T., Combined Production of *tert*-Amyl Methyl Ether and Higher Ethers Using Catalytic Distillation, *Proceedings of the 5th World Congress of Chemical Engineering Vol III*, AIChE, New York 1996, 1071.

Koskinen, M., Järvelin, H., Lindqvist, P., NexETHERS – New way of producing ethers, *Seventh EFOA Conference*, Brussels 1996.

Krishnamurthy R. and Taylor R., A nonequilibrium stage model of multicomponent separation processes. Part I: model description and method of solution, *AIChE J.* **31** (1985) 449-445.

Landon, V.G. Temperature Correction for Packed Bed Multitubular Reactors with Concentric Axial Thermowells, *Computers Chem. Engng.* **20** (1996) 475.

Legawiec, B. and Ziolkowski, D. Mathematical Simulation of Heat Transfer Within Tubular Flow Apparatus with Packed Bed by a Model Considering System Homogeneity, *Chem. Eng. Sci.* **50** (1995) 673.

Leu, A.-D. and Robinson, D.B., High Pressure Vapor-Liquid Equilibrium Phase Properties of the Isopentane-Hydrogen Sulfide and Neopentane-Hydrogen Sulfide Binary Systems, *J. Chem. Eng. Data* **37** (1992) 10.

Lievo, P., Almark, M., Purola, V.-M., Pyhalahti, A. and Aittamaa, J. Miniplant, effective means to develop and design new processes, *Annual Meeting Archive - American Institute of Chemical Engineers*, Indianapolis 2002, 2010.

Marchionna, M., Di Girolamo, M. and Patrini, R., Light olefins dimerization to high quality gasoline components, *Catal. Today* **65** (2001) 397.

Martin, H., Low Peclet number particle-to-fluid heat and mass transfer in packed beds, *Chem. Eng. Sci.* **33** (1978) 913.

Matouq, M. H. and Goto, S., Kinetics of Liquid-Phase Synthesis of Methyl tert-Butyl Ether from tert-Butyl Alcohol and Methanol Catalyzed by Ion Exchange Resin, *Int. J. Chem. Kinet*. **25** (1993) 825.

Mazzotti, M., Kruglow, A., Neri, B., Gelosa, D. and Morbidelli, M., A continuous chromatographic reactor: SMBR., *Chem. Eng. Sci.* **51** (1996) 1827.

Morse, P. M., Producers Brace for MTBE Phaseout, *Chem. Eng. News* **77** (1999) 26.

Nelder J.A. and Mead R., A simplex method for function minimization, *Comp. J.* **7** (1965) 308.

Perry, R.H. and Green, D.W. *Perry's Chemical Engineers' Handbook*, 7th ed., McGraw-Hill, New York 1997.

Pilipenko, I.B., Chaplits, D.N., Balashov, M.I. and L'vov, S.V. Liquid-liquid phase equilibrium in butylene-water-trimethylcarbinol systems. *Fiz.-Khim. Osn. Rektifikatsii* (1970) 368.

Pyhälahti A., *Reactive Distillation in Literature,* Helsinki University of Technology, Laboratory of Chemical Engineering, Plant Design Report Series, Report no. 42, Espoo 1996.

Reid R.C., Prausnitz, J.M. and Poling B.E., *The Properties of Gases and Liquids*, 4th Ed., McGraw-Hill, New York 1987.

Rihko, L. K., Kiviranta-Pääkkönen , P. K. and Krause , A. O. I., Kinetic Model for the Etherification of Isoamylenes with Methanol, *Ind. Eng. Chem. Res*. **36** (1996) 614-621.

Rihko, L.K. , Linnekoski, J. A., Krause A.O.I., Reaction Equilibria in the Synthesis of 2-Methoxy-2-Methylbutane and 2-Ethoxy-2-Methylbutane in the Liquid Phase, *J. Chem. Eng. Data* **39** (1994) 700-704.

Scharfe, G., Convert butenes to high octane oligomers, *Hydrocarbon Process.* **52** (1973) 171.

Schlünder, E.U., On the mechanism of mass transfer in heterogeneous systems – in particular in fixed beds, fluidized beds and on bubble trays, *Chem. Eng. Sci.* **32** (1977) 845.

Schwartz, C.E. and Smith, J.M., Flow distributions in packed beds, *Ind. Engng. Chem.* **45** (1953) 1209.

Sloan, H.D., Birkhoff, R., Gilbert, M.F., Nurminen, M., Pyhälahti, A., Isooctane production from C4's as an alternative to MTBE, *NPRA 2000 Annual meeting*, San Antonio 2000.

Stankiewicz, A., Advances in Modeling and Design of Multitubular Fixed-Bed Reactors, *Chem.Eng.Technol.* **12** (1989) 113.

Sundmacher, K., and U. Hoffmann, Development of a New Catalytic Distillation Process for Fuel Ethers via a Detailed Nonequilibrium Model, *Chem. Eng. Sci.* **51** (1996) 2359.

Taylor, R. and Krishna, R., Modelling Reactive Distillation, *Chem.Eng.Sci.* **55** (2000) 5183.

Taylor, R., Kooijman, H. A. and Hung, J.-S., A second generation nonequilibrium model for computer simulation of multicomponent separation processes, *Comp. Chem. Engng* **18** (1994) 205.

Tejero, J., Caldero´n, A., Cunill, F., Izquierdo, J. F. and Iborra, M., The Formation of Byproducts in the Reaction of Synthesis of Isopropyl *tert*-Butyl Ether from Isopropyl Alcohol and Isobutene on an Acidic Macroporous Copolymer, *React. Funct. Polym.* **33** (1997) 201.

Thomson, G.H., Brobst, K.R., and Hankinson, R.W., An Improved. Correlation for Densities of Compressed Liquids and Liquids Mixtures, *AIChE J.* **28** (1982) 671-676.

Uusi-Kyyny, P., Pokki, J.-P., Aittamaa, J. and Liukkonen, S., Vapor-Liquid Equilibrium for the Binary Systems of Methanol +2,4,4-Trimethyl-1-pentene at 331 K and 101 kPa and Methanol +2-Methoxy-2,4,4-trimethylpentane at 333 K, *J. Chem. Eng. Data* **46** (2001) 1244.

Uusi-Kyyny, P., Pokki, J.-P., Laakkonen, M., Aittamaa, J. and Liukkonen, S., Vapor liquid equilibrium for the binary systems 2-methylpentane + 2-butanol at 329.2 K and n-hexane + 2-butanol at 329.2 and 363.2 K with a static apparatus, *Fluid Phase Equilib.* **201** (2002) 343-358.

Velo, E., Puigjaner, L. and Recasens, F., Intraparticle Mass Transfer in the Liquid-Phase Hydration of Isobutene: Effects of Liquid Viscosity and Excess Product, *Ind. Eng. Chem. Res*. **29** (1990) 1485.

Verrazzi,V., Kikic, I., Garbers, P., Barreau, A. and Le Roux, D., Vapor-Liquid Equilibrium in Binary Systems Ethanol+C4 and C5 Hydrocarbons, *J. Chem. Eng. Data* **43** (1998) 949-953.

Vila, M., Cunill, F., Izquierdo, J.-F., Gonzalez, J. and Hernandez, A., The Role of By-Products Formation in Methyl *tert*-Butyl Ether Synthesis Catalyzed by a Macroporous Acidic Resin, *Appl.Catal.A* **117** (1994) L99.

Weidlich, U. and Gmehling, J. A., modified UNIFAC model. 1. Prediction of VLE, HE, and g^E, *Ind. Eng. Chem. Res.* **26** (1987) 1372.

Wilson, G.M., Vapor-liquid equilibrium. XI. A new expression for the excess free energy of mixing, *J. Am. Chem. Soc*. **86** (1964) 127.

Winterberg, M. and Tsotsas, E., Modelling of heat transport in beds packed with spherical particles for various bed geometries and/or thermal boundary conditions, *Int.J.Therm.Sci.* **39** (2000) 556.

Yaws, C.L., *Chemical Properties Handbook*, McGraw-Hill, New York 1999.

Yin, X., Yang, B. and Goto, S., Kinetics of Liquid-Phase Synthesis of Ethyl tert-Butyl Ether from tert-Butyl Alcohol and Ethanol Catalyzed by Ion Exchange Resin and Heteropoly Acid, *Int. J. Chem. Kinet.* **27** (1995) 1065.

Zabaloy, M.-S., Gros, H.P., Bottini, S.B. and Brignole E.A., Isothermal Vapor-Liquid Equilibrium Data for the Binaries Isobutane-Ethanol, Isobutane-1-Propanol, and Propane-Ethanol, *J. Chem. Eng. Data* **39** (1994) 214.

Zehner, P. and Schluender, E., Thermal conductivity of packings at moderate temperatures, *Chem.Eng.Tech.* **42** (1970) 933.

NOTATION

$\varnothing$ = diameter, m

a_i = activity of component i

ASOG = analytical solution of groups

C_i = concentration of component I, mol/m^3

c_P = heat capacity of the reactor fluid, J/mol·K

$c_{P.heat}$ = heat capacity of the heat transfer fluid, J/kg·K

CSTR = continuously stirred tank reactor

D_{er} = effective radial diffusivity, m^2/s

d_{ext} = external diameter of the reactor tube, m

d_i = external diameter of the thermowell, m

DIPPR = the design institute for physical properties

d_o = internal diameter of the reactor tube, m

d_P = catalyst diameter, m

$d_{p,ave}$ = average catalyst diameter, average particle size, m

d_R = reactor tube diameter, m

E_i = activation energy of the Arrhenius equation, kJ mol^{-1}

ETBE = Ethyl tert-butyl ether

F = preexponential factor of the Arrhenius equation (eq 3), mol s^{-1} kg$_{cat}^{-1}$

FCC = Fluid catalytic cracking

F-factor = vapor kinetic energy term, m/s(kg/m^3)^{½}

F_{ref} = preexponential factor of reparametrized Arrhenius equation, mol s^{-1} kg $_{cat}^{-1}$

GC = gas chromatograph

ΔH_r = enthalpy of reaction, J/mol

$\dot{H}_i$ = enthalpy flow in layer i, J/mol·s

HETP = height equivalent to a theoretical plate / m

IB = diisobutene, 2,4,4-trimethyl pentene

IB = isobutene, 2-methylpropene

IP = isopentane, 2-methylbutane

k = reaction rate constant, mol s^{-1} kg_{cat}^{-1}

LLE = liquid-liquid equilibrium

l_R = reactor length, m

$\dot{m}_{heat}$ = mass flow of the heat transfer fluid, kg/s

MeOAc = Methyl acetate

MON = motor octane number

MTBE = methyl tert-butyl ether, 2-methoxy-2-methyl propane

NTU = number of transfer units

p = pressure, Pa

Pr = Prandtl number, $Pr = \mu \cdot c_P / \lambda_g$

R = radius, m

RD = Reactive distillation

Re_p = Reynolds number, based on the surface velocity of the fluid, $Re_p = \rho_g \cdot v \cdot d_p / \mu$

r_i = reaction rate of component i, mol s^{-1} kg_{cat}^{-1}

R_o = reactor tube inside radius, m

RON = research octane number

RPA = Reactive Pump Around Concept

SRC = Side reactor concept

T = temperature, K

TAEE = Tert-amyl ethyl ether

TAME = Tertiary amyl-methyl ether

TBA = tert-butyl alcohol, 2-methyl-2-propanol

T_{heat} = temperature of the heating fluid, K

TMP-1 = 2,4,4-trimethyl-1-pentene, diisobutene, DIB

T_{ref} = reference temperature of reparametrized Arrhenius equation, K

TRIB = triisobutene

T_{wall} = temperature of the reactor tube wall, K

UNIFAC = universal quasi-chemical functional group activity coefficient

V_i^L = pure component molar volume for component i, m^3/mol

VLE = vapour-liquid equilibrium

VLLE = vapour-liquid-liquid equilibrium

v_t = vapor superficial velocity, m/s

x_{az} = azeotropic molar fraction of a component

x_i = molar fraction of component i

GREEK LETTERS

α_{hw} = heat transfer coefficient between heating fluid and reactor wall, $W/m^2 \cdot K$

α_w = wall heat transfer coefficient, $W/m^2 \cdot K$

Δ = difference

ε = local porosity of the catalyst bed

ε_{ave} = average porosity of the catalyst bed

λ_{cat} = thermal conductivity of the catalyst, W/m·K

λ_{er} = effective radial thermal conductivity, W/m·K

λ_{er}^0 = static contribution to the effective radial thermal conductivity, W/m·K

λ_{er}^t = dynamic contribution to the effective radial thermal conductivity, W/m·K

λ_g = thermal conductivity of the reaction fluid, W/m·K

λ_{ij} = binary interaction parameter in Wilson equation between components i and j, J/mol

Λ_{ij} = binary interaction parameter for components i and j

γ_i = activity coefficient of component i

μ = viscosity of the fluid, kg/m·s

ρ_B = bulk density of the catalyst in the reactor, kg/m^3

ρ_g = density of the reaction fluid, kg/m^3

ISBN 951-22-7925-8
ISSN 1236-875X